Article

Analysis of the Genome of the Heavy Metal Resistant and Hydrocarbon-Degrading Rhizospheric *Pseudomonas qingdaonensis* ZCR6 Strain and Assessment of Its Plant-Growth-Promoting Traits

Daria Chlebek [ID]**, Tomasz Płociniczak** [ID]**, Sara Gobetti, Agata Kumor** [ID]**, Katarzyna Hupert-Kocurek** [ID]
and Magdalena Pacwa-Płociniczak * [ID]

Institute of Biology, Biotechnology and Environmental Protection, Faculty of Natural Sciences, University of Silesia in Katowice, Jagiellońska 28, 40-032 Katowice, Poland; dachlebek@us.edu.pl (D.C.); tomasz.plociniczak@us.edu.pl (T.P.); sara.gobetti@edu.unito.it (S.G.); agata.kumor@us.edu.pl (A.K.); katarzyna.hupert-kocurek@us.edu.pl (K.H.-K.)
* Correspondence: magdalena.pacwa-plociniczak@us.edu.pl; Tel.: +48-322009442

Abstract: The *Pseudomonas qingdaonensis* ZCR6 strain, isolated from the rhizosphere of *Zea mays* growing in soil co-contaminated with hydrocarbons and heavy metals, was investigated for its plant growth promotion, hydrocarbon degradation, and heavy metal resistance. In vitro bioassays confirmed all of the abovementioned properties. ZCR6 was able to produce indole acetic acid (IAA), siderophores, and ammonia, solubilized $Ca_3(PO_4)_2$, and showed surface active properties and activity of cellulase and very high activity of 1-aminocyclopropane-1-carboxylic acid deaminase (297 nmol α-ketobutyrate $mg^{-1} h^{-1}$). The strain degraded petroleum hydrocarbons (76.52% of the initial hydrocarbon content was degraded) and was resistant to Cd, Zn, and Cu (minimal inhibitory concentrations reached 5, 15, and 10 mM metal, respectively). The genome of the ZCR6 strain consisted of 5,507,067 bp, and a total of 5055 genes were annotated, of which 4943 were protein-coding sequences. Annotation revealed the presence of genes associated with nitrogen fixation, phosphate solubilization, sulfur metabolism, siderophore biosynthesis and uptake, synthesis of IAA, ethylene modulation, heavy metal resistance, exopolysaccharide biosynthesis, and organic compound degradation. Complete characteristics of the ZCR6 strain showed its potential multiway properties for enhancing the phytoremediation of co-contaminated soils. To our knowledge, this is the first analysis of the biotechnological potential of the species *P. qingdaonensis*.

Keywords: rhizospheric bacteria; *Pseudomonas qingdaonensis*; plant growth promotion; hydrocarbons; heavy metals; biosurfactants; genome mining

1. Introduction

Due to the widespread contamination of the environment with petroleum hydrocarbons and heavy metals posing a critical threat to human health and the environment, finding innovative ways to remove these pollutants has become a priority in the remediation field. One of the most promising strategies is phytoremediation assisted by rhizobacteria and endophytes that are known to promote plant growth and development through various mechanisms, such as the synthesis of phytohormones, lowering the level of ethylene, facilitating the uptake of minerals, increasing the bioavailability of pollutants through the synthesis of surfactants, and, most importantly, reducing the toxicity of organic contaminants through their enzymatic mineralization [1–5]. It was suggested that cooperation between plant-growth-promoting bacteria and hydrocarbon-/heavy-metal-tolerant plants may result in more effective phytoremediation of soil co-contaminated with these compounds [6].

Literature data indicate the clear potential of *Pseudomonas* strains to participate in restorative phytoremediation of polluted areas, which will enhance sustainable agricultural

production and environmental protection [7,8]. Among plant-associated bacteria, *Pseudomonas* strains are capable of metabolizing a wide range of hydrocarbons. For example, *Pseudomonas* sp. Ph6 tested by Sun et al. [9] was able to degrade phenanthrene with 81.1% efficiency, whereas the *Pseudomonas* sp. P3 strain used by Zhu et al. [10] showed high potential to degrade naphthalene, phenanthrene, fluorene, pyrene, and benzo(a)pyrene. Several works have also demonstrated the ability of *Pseudomonas* members to degrade crude oil [11]. The positive effect of these microorganisms on plants exposed to stressful conditions is determined by an improvement in their viability and an increase in biomass. The inoculation of two species of willow (*Salix purpurea* and *Salix discolor*) and perennial ryegrass (*Lolium perenne*) with *Pseudomonas putida* PD1 promoted root and shoot growth and protected the plants against the phytotoxic effect of phenanthrene. Furthermore, 25 to 40% removal of xenobiotics from the soil was observed [12]. In turn, the application of *Pseudomonas putida* VM1450 for the clean-up of soil polluted with 2,4-dichlorophenoxyacetic acid resulted in the increased removal of this herbicide from soil and its reduced accumulation in plant tissues [13]. Bakaeva et al. [14] demonstrated that treating barley seeds with strains of the *Pseudomonas* genus increased germination and root growth in soil contaminated with petroleum oil. Apart from the capability of organic xenobiotic utilization and plant growth promotion, some rhizospheric *Pseudomonas* show resistance to heavy metals and possess features that can alter metal bioavailability, which makes them a useful tool in the remediation of heavy-metal-polluted environments [15,16]. These bacteria contribute to the mobilization and uptake of heavy metals by plants and improve plant growth under heavy metal exposure. For example, Płociniczak et al. [17] noted an increase in Zn and Cd accumulation in the shoot tissues of *Silene vulgaris* by 43.8% and 112.6%, respectively, in plants inoculated with *Pseudomonas helmanticensis* H16 compared to control plants treated with bacterial necromass. It is worth emphasizing that *Pseudomonas* species can adapt to various environmental conditions due to abundant genetic diversity [18]. However, knowledge about genome plasticity remains limited. The application of high-throughput sequencing techniques and functional genomics provides a new direction to achieve a deeper understanding of the genetic basis for versatile metabolic potential and environmental adaptation [19].

In this study, a new *Pseudomonas qingdaonensis* ZCR6 strain isolated from the rhizosphere of *Zea mays* growing in soil co-contaminated with hydrocarbons and heavy metals was investigated, and its plant-growth-promoting traits along with its ability to degrade hydrocarbons and resist heavy metals were investigated.

To the best of our knowledge, there is no previous report on rhizosphere-associated *P. qingdaonensis* with the characteristics of hydrocarbon degradation, heavy metal resistance, biosurfactant production, and plant growth promotion.

2. Results and Discussion

2.1. Isolation and Identification of the Isolate

The isolation and selection of plant-growth-promoting, hydrocarbon-degrading, and heavy-metal-resistant bacteria from the rhizosphere of plants seems to be particularly important for exploiting the bioremediation potential of plant-bacteria systems [11]. In this study, bacterial strain ZCR6 was isolated as one of 26 strains from the rhizosphere of *Zea mays* growing in soil co-contaminated with hydrocarbons and heavy metals in the vicinity of the Coke Plant "Jadwiga" in Zabrze (Upper Silesia, Poland). Among the isolates, the ZCR6 strain showed the highest ACC deaminase activity, very high surface-active and emulsification activity, demonstrated an ability to produce IAA, siderophores, ammonia, and cellulase, and solubilized $Ca_3(PO_4)_2$ (Table 1). Based on these results, the ZCR6 strain, as the most promising strain, was chosen for further characterization. Phylogenetic analyses showed that the ZCR6 strain is closely related to *Pseudomonas qingdaonensis* JJ3[T], an aflatoxin-degrading bacterium isolated from peanut rhizospheric soil, the taxonomic name of which is not validated yet (Figure 1) [20]. According to the EZBioCloud database, the closest relatives of strain ZCR6 (OK597188), on the basis of the 16S rRNA gene se-

quence, were *Pseudomonas qingdaonensis* JJ3[T] (100%, MG589917), *Pseudomonas brassicae* MAFF 212427[T] (99.86%, LC514379), and *Pseudomonas defluvii* WCHP16[T] (99.29%, KY979145) (Supplementary Figure S1). In the MLSA, the sequence length of three concatenated genes after alignment was 2563 bp. Through the analysis of concatenated 16S rRNA and two housekeeping genes, ZCR6 was placed into the *P. putida* subgroup [21]. For the ZCR6 strain, the highest average nucleotide identity was observed for *P. qingdaonensis* (99.95%), *P. brassicae* (97.30%), and *P. laurentiana* (95.95%) (Figure 1). The genomic comparison using the TrueBac ID tool showed 99.18% similarity between the genomes of the ZCR6 and *P. qingdaonensis* JJ3[T] strains.

Table 1. The activity of the plant-growth-promoting mechanisms and surface-active abilities of the ZCR6 strain.

ACCD [a]	IAA [b]	Ca$_3$(PO$_4$)$_2$ [c]	Siderophore [d]	HCN [e]	NH$_3$ [f]	CMC [g]	Surface Tension [h]	Oil-Spreading [i]	H [k]	X [l]	D [m]
PGP Mechanisms						**Plant Colonisation**	**Surface-Active Properties**			**Emulsification Index [j]**	
296.73 ± 1.27	3.59 ± 0.11	6.5 ± 0.53	+	-	+	+	68.1 ± 0.55	4.0 ± 0.2	25.71 ± 0.57	71.43 ± 1.43	14.71 ± 0.29

[a] ACCD activity (nmol a-ketobutyrate mg^{-1} h^{-1}); [b] (IAA mL^{-1} of medium); [c] the halo diameter (mm) calculated by subtracting the colony diameter from the total halo size; [d–g] + positive; − negative; [h] (mN m^{-1}); [i] (mm); [j] (%); [k] H—*n*-hexadecane; [l] X—*p*-xylene; [m] D—diesel oil.
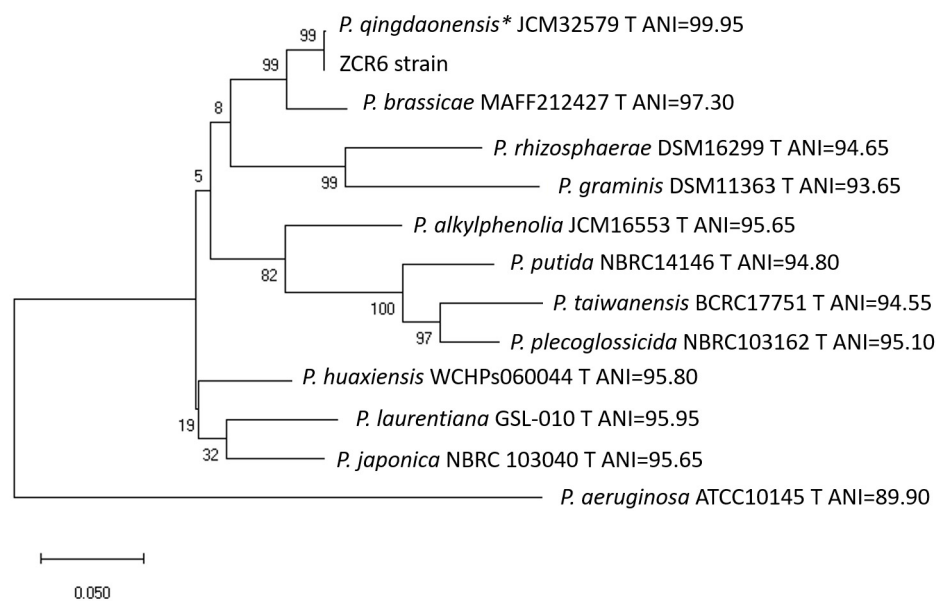

Figure 1. Maximum-likelihood-based phylogeny resulting from the concatenated 16S rRNA, *gyrB*, and *rpoD* sequences, representing the relative position of the ZCR6 strain among other *Pseudomonas*. All positions containing gaps or missing data were eliminated. The final dataset contained 2563 positions. Accession numbers of sequences used in this study are listed in Supplementary Table S1. Bootstrap values are represented at the branching points. The bar represents 0.05 substitutions per site. Each strain is given an ANI value relative to the sequences belonging to the ZCR6 strain; * strain JJ3[T] with the highest ANI value.

To our knowledge, little is known about the *P. qingdaonensis* strains associated with plants in the context of their use in environmental biotechnology. Therefore, the presented research will help to expand our knowledge about this species, recently isolated for the first time by Wang et al. [20].

2.2. Biochemical Characteristics and Cellular Fatty Acid Composition of the ZCR6 Strain

The biochemical characteristics revealed that *P. qingdaonensis* ZCR6 was positive for oxidase, catalase, and arginine dihydrolase, and was able to produce pyoverdine. In turn, it

was negative for dehydrogenase, urease, nitrate reductase, and gelatinase, and was unable to hydrolyze starch and produce pyocyanin. The obtained results were consistent with those obtained in [20] for the *P. qingdaonensis* strain JJ3[T], except for its starch hydrolysis ability and the production of pyoverdine; however, these may be due to natural variability between strains belonging to the same species.

The cellular fatty acid composition of the ZCR6 strain showed a high percentage of C16:0 (30.98%), C16:1ω7c/C16:1ω6c (26.35%), C18:1ω7c/C18:1ω6c (15.44%), and C17:0 cyclo (10.22%) fatty acids. Additionally, the hydroxylated fatty acids C12:0 2OH, C12:0 3OH, and C10:0 3OH were detected, and their abundance was in the range of 3.34–4.63%. Moreover, C12:0 and C19:0 cyclo ω8c fatty acids were present; however, their abundance was low, 2.22% and < 1%, respectively (Table 2). These results differed from the profile obtained for the JJ3[T] strain, which was dominated by C17:0 cyclo (24%) and C16:0 (21.4%), while C16:1ω7c/C16:1ω6c and C18:1ω7c/C18:1ω6c fatty acids constituted only 11.5% and 10.5% of the total fatty acids, respectively [20]. However, Wang et al. [20] used a three-day-old culture instead of a 24-h-old culture, as is required and recommended in the MIDI-MIS method. To compare our results with JJ3[T] strain fatty acid methyl esters (FAMEs), analysis of three-day-old ZCR6 culture was performed. The obtained results showed a high similarity of both profiles.

Table 2. Fatty acid composition (%) of the ZCR6 strain.

	Percentage (%)	
	24 h	**72 h**
C16:0	30.95	22.52
C16:1ω7c and/or C16:1ω6c	26.35	11.42
C18:1ω7c and/or C18:1ω6c	15.44	11.68
C17:0 cyclo	10.22	23.07
C12:0 2OH	4.63	8.74
C12:0 3OH	4.11	7.57
C10:0 3OH	3.34	4.35
C12:0	2.22	4.07
C 19:0 cyclo ω8c	<1	5.14
Others	<2	<2

2.3. General Features of the Genome

Genome analysis was performed to characterize the genetic potential of this bacterium.

To the best of our knowledge, this is the first study performing a genome analysis of *P. qingdaonensis* species isolated from the rhizosphere of maize. The genome of *P. qingdaonensis* ZCR6 was assembled into 52 contigs consisting of 5,507,067 bp with an average G + C content of 64.5%. Previously, similar genome sizes of different *Pseudomonas* species isolated from the rhizosphere of various plants were reported [20,22,23]. A total of 5055 genes were annotated in the genome, of which 4943 were protein-coding sequences (CDSs). Furthermore, 8 rRNA-, 64 tRNA-, and 4 ncRNA-encoding genes were predicted. A large number of rRNAs is a typical characteristic of microorganisms, allowing them to respond rapidly to changing nutrient availability [24]. In addition, two intact prophage regions of 21.7 kb and 5.9 kb with GC contents of 62.29% and 60.54%, respectively, were identified. It is worth emphasizing that the presence of a prophage in the bacterial genome may increase its resistance to environmental stresses and biofilm formation and support horizontal gene transfer [25]. The general genome features of the ZCR6 strain are described in Table 3. The circular genome representing the entire genome assembly is shown in Figure 2.

Table 3. Genome features of *P. qingdaonensis* ZCR6.

Feature	Value
Assembly information	
Genome size (bp)	5,507,067
Contigs	52
Conting N50 (bp)	292,270
Conting L50	7
G + C content (%)	64.5
Annotation information	
Genes (total)	5055
CDSs (total)	4979
Genes (coding)	4943
CDSs (with protein)	4943
Pseudogenes	36
RNA genes	76
rRNA	3, 3, 2 (5S, 16S, 23S)
tRNA	64
ncRNA	4
Prophage regions	2
Genes assigned to KEGG pathways	2945
Genes assigned to KEGG Orthology (KO)	2209
Genes assigned to COGs	4877
Genes connected to RASTtk	2319
BioProject ID	PRJNA681194
BioSample ID	SAMN16935590
GeneBank accession number	JADWSX000000000

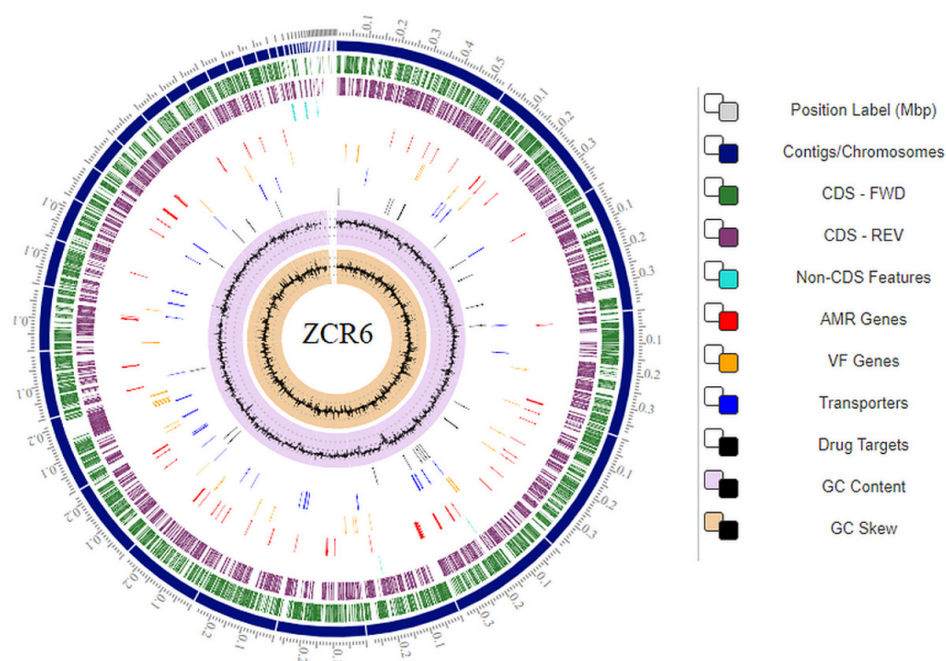**Figure 2.** Circular plot representing the genome annotations of the ZCR6 strain. Colors depict the different classification types of gene clusters along the sequenced genome. The description of each circle is represented from the outermost circle to the innermost circle. Tick marks represent the predicted CDS on the positive and negative strands. AMR—antimicrobial resistance genes; VF—virulence factor genes.

The COG database was used to functionally categorize predicted proteins. A total of 4877 protein-encoding genes in the ZCR6 strain were assigned to COG in 21 functional categories (Figure 3). This analysis revealed the highest gene abundance for amino acid transport and metabolism (E, 9.47%), transcription (K, 9.37%), inorganic ion transport (P, 8.35%), signal transduction mechanisms (T, 6.62%), energy production and conversion (C, 6.48%), and cell wall/membrane/envelope biogenesis (M, 6.15%). It is worth noting that the high percentage of genes belonging to the E and P classes may suggest the innate ability of the ZCR6 strain to compete with other microorganisms. It is also worth noting that the high metabolic activity of the studied strain may be reflected in the occurrence of many genes involved in the transcription process [25,26]. Genes belonging to the E and K categories constitute the largest group of genes for other well-known plant growth promotors, *P. fluorescens* PICF7 and *Pseudomonas* sp. UW4 [27,28]. The functional annotation performed using KEGG identified 2945 associated genes (Figure 3). The largest fraction of the predicted genes was assigned to the metabolism of amino acids (327 genes, 11.1%) and carbohydrates (282 genes, 9.57%), as well as to environmental and information processing: membrane transport (146 genes, 4.96%) and signal transduction (140 genes, 4.75%) (Figure 4A). The annotated genes were also assigned and grouped into subsystem feature categories. A clear advantage in the percentage of genes was noted for metabolism cofactors and vitamins (305 genes, 10.4%), amino acids and derivatives (298 genes, 10.2%), protein synthesis (179 genes, 6.14%), and membrane transport (174 genes, 5.9%) (Figure 4B). These results confirmed a preference consistent with the previous results from COG and KEGG functional analysis.
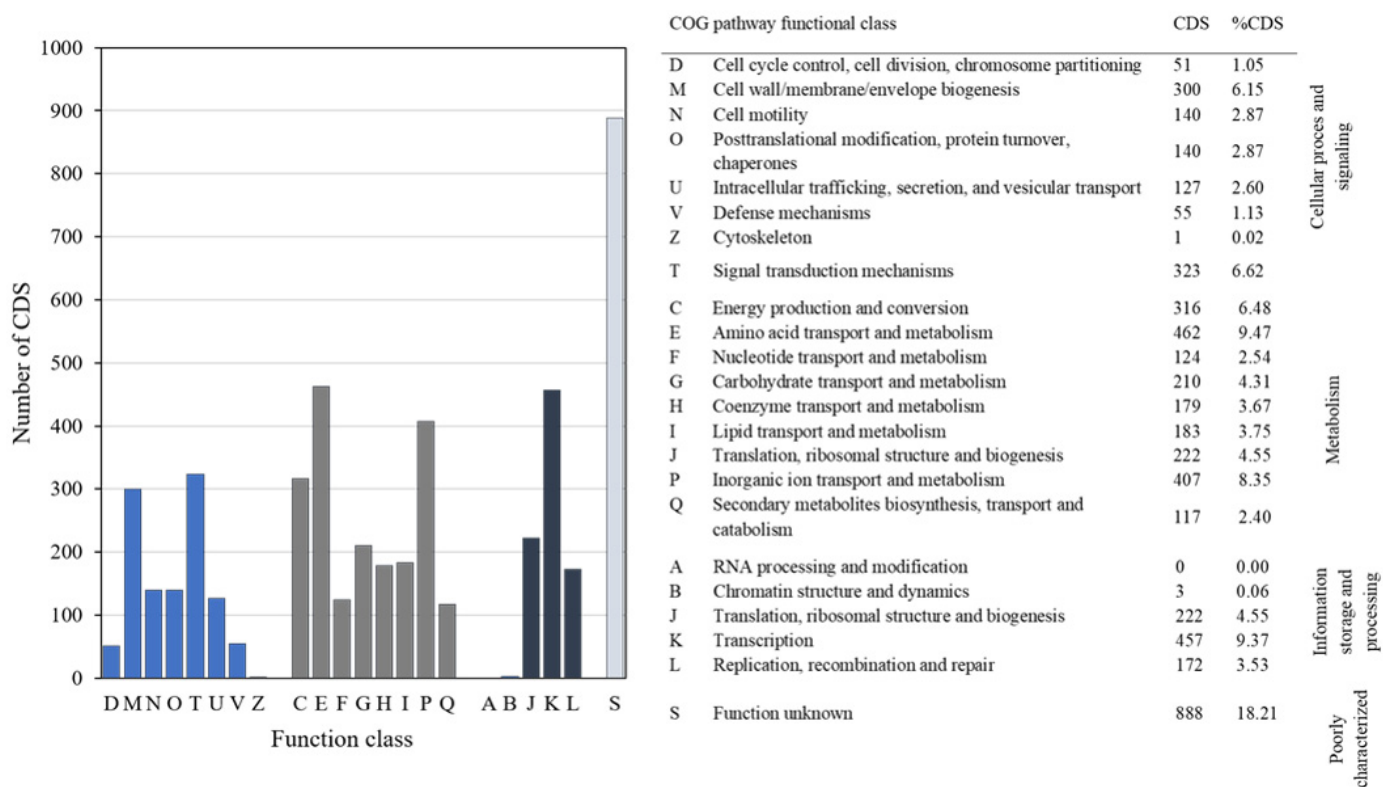

COG pathway functional class		CDS	%CDS	
D	Cell cycle control, cell division, chromosome partitioning	51	1.05	Cellular proces and signaling
M	Cell wall/membrane/envelope biogenesis	300	6.15	
N	Cell motility	140	2.87	
O	Posttranslational modification, protein turnover, chaperones	140	2.87	
U	Intracellular trafficking, secretion, and vesicular transport	127	2.60	
V	Defense mechanisms	55	1.13	
Z	Cytoskeleton	1	0.02	
T	Signal transduction mechanisms	323	6.62	
C	Energy production and conversion	316	6.48	Metabolism
E	Amino acid transport and metabolism	462	9.47	
F	Nucleotide transport and metabolism	124	2.54	
G	Carbohydrate transport and metabolism	210	4.31	
H	Coenzyme transport and metabolism	179	3.67	
I	Lipid transport and metabolism	183	3.75	
J	Translation, ribosomal structure and biogenesis	222	4.55	
P	Inorganic ion transport and metabolism	407	8.35	
Q	Secondary metabolites biosynthesis, transport and catabolism	117	2.40	
A	RNA processing and modification	0	0.00	Information storage and processing
B	Chromatin structure and dynamics	3	0.06	
J	Translation, ribosomal structure and biogenesis	222	4.55	
K	Transcription	457	9.37	
L	Replication, recombination and repair	172	3.53	
S	Function unknown	888	18.21	Poorly characterized

Figure 3. COG classification of predicted genes in the ZCR6 strain. Colored bars indicate the CDS assigned to each COG category.
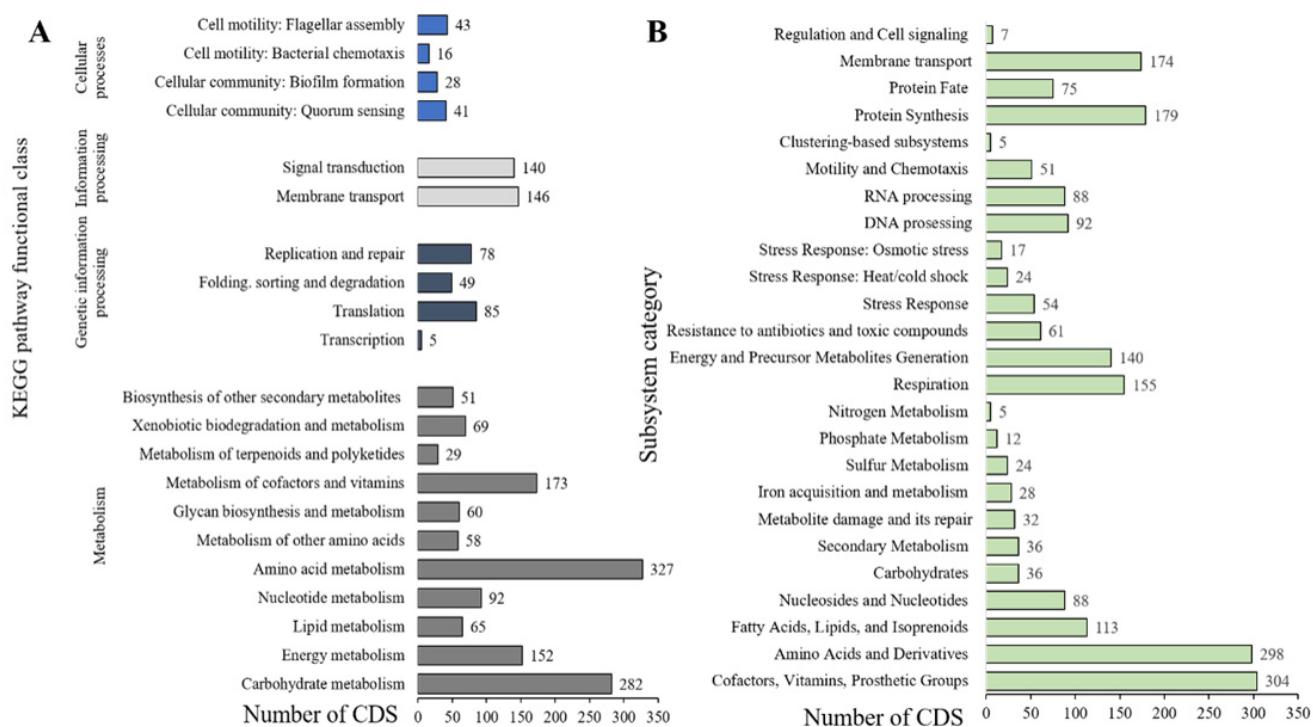
Figure 4. KEGG pathway classification of predicted genes in the ZCR6 strain using KEGG BlastKoala (**A**). Protein-coding sequences grouped into the functional subsystems in the ZCR6 genome using RASTtk (**B**).

2.4. Plant Growth Promotion Potential

2.4.1. Nutrient (N, P, S, Fe) Acquisition

Rhizospheric bacteria use various mechanisms of action to stimulate plant growth. First, due to their direct vicinity of plant roots, they enhance the bioavailability and uptake of beneficial nutrients, such nitrogen (N), phosphorus (P), and sulfur (S). N is an essential nutrient for plant growth, development, and reproduction; however, plants are unable to utilize atmospheric nitrogen (N_2). Fortunately, some rhizospheric bacteria, called diazotrophs, are able to convert N_2 to ammonia (NH_3) in a process called biological nitrogen fixation (BNF) using a complex system known as nitrogenase [5]. Among diazotrophs, the *Azotobacter, Azospirillum, Rhizobium*, and *Bradyrhizobium* genera are the best known [29]; however, species of *Pseudomonas* (e.g., *Pseudomonas stutzeri*) have also been reported [30,31]. The genome of the ZCR6 strain lacks a full set of genes necessary for nitrogen fixation. Nevertheless, the presence of *iscS* and *iscU* genes encoding cysteine desulfurase and nitrogen fixation protein, respectively, with a primary sequence similar to those of NifS and NifU proteins, was reported (Table 4). The role of NifS and NifU is the formation of iron–sulfur (Fe–S) clusters required for the maturation of nitrogenase in nitrogen-fixing microorganisms [32]. Because it was found that functional cross talk between the Nif and ISC systems is possible [33], NifS- and NifU-like proteins from the ZCR6 strain may have been engaged in the formation of Fe–S clusters by other nitrogen-fixing rhizobacteria when the loss of neither NifS nor NifU function occurred. The ZCR6 strain was not able to fix atmospheric nitrogen but showed the ability to produce ammonia (probably via ACCD activity) (Table 1). This mechanism of PGP may also support plant growth by facilitating better supplementation of plants with assimilable forms of N.

Table 4. Products of the genes involved in the most important plant growth promotion traits present in the genome of the ZCR6 strain.

Gene	Accession Number	KO Number	Gene Product	Activity
iscS	MBG8561789.1	K04487	Cysteine desulfurase	Nitrogen fixation
iscU	MBG8560681.1	K04488	Nitrogen fixation protein nifu	
gcd	MBG8562075.1	K00117	Quinoprotein glucose dehydrogenase (EC:1.1.5.2)	Phosphate solubilization
pqqA	MBG8558041.1	K06135	Pyrroloquinoline quinone biosynthesis protein A	
pqqB	MBG8558042.1	K06136	Pyrroloquinoline quinone biosynthesis protein B	
pqqC	MBG8558043.1	K06137	Pyrroloquinoline-quinone synthase (EC:1.3.3.11)	
pqqD	MBG8558044.1	K06138	Pyrroloquinoline quinone biosynthesis protein D	
pqqE	MBG8558045.1	K06139	Pqqa peptide cyclase (EC:1.21.98.4)	
ppa	MBG8560327.1	K01507	Inorganic pyrophosphatase (EC:3.6.1.1)	
ppx-gppA	MBG8558276.1	K01524	Exopolyphosphatase/guanosine-5′-triphosphate,3′-diphosphate pyrophosphatase (EC:3.6.1.11 3.6.1.40)	
pstB	MBG8558408.1	K02036	Phosphate transport system ATP-binding protein (EC:7.3.2.1)	
pstA	MBG8558409.1	K02038	Phosphate transport system permease protein	
pstC	MBG8558410.1	K02037	Phosphate transport system permease protein	
pstS	MBG8558411.1	K02040	Phosphate transport system substrate-binding protein	
pit	MBG8560129.1	K16322	Low-affinity inorganic phosphate transporter	
phoB	MBG8558402.1	K07657	Two-component system. Ompr family. Phosphate regulon response regulator phob	
phoR	MBG8558403.1	K07636	Two-component system. Ompr family. Phosphate regulon sensor histidine kinase phor (EC:2.7.13.3)	
phoU	MBG8558407.1	K02039	Phosphate transport system protein	
ssuA	MBG8561374.1	K15553	Sulfonate transport system substrate-binding protein	Sulfur metabolism
ssuB	MBG8560999.1	K15555	Sulfonate transport system ATP-binding protein (EC:7.6.2.14)	
ssuC	MBG8561372.1	K15554	Sulfonate transport system permease protein	
ssuD	MBG8561373.1	K04091	Alkanesulfonate monooxygenase (EC:1.14.14.5)	
ssuE	MBG8561375.1	K00299	FMN reductase (EC:1.5.1.38)	
cysP	MBG8561508.1	K02048	Sulfate/thiosulfate transport system substrate-binding protein	
cysU	MBG8561415.1	K02046	Sulfate/thiosulfate transport system permease protein	
cysW	MBG8561414.1	K02047	Sulfate/thiosulfate transport system permease protein	
cysA	MBG8561413.1	K02045	Sulfate/thiosulfate transport system ATP-binding protein (EC:7.3.2.3)	
cysI	MBG8558903.1	K00381	Sulfite reductase (NADPH) hemoprotein beta-component (EC:1.8.1.2)	
cysJ	MBG8560698.1	K00380	Sulfite reductase (NADPH) flavoprotein alpha-component (EC:1.8.1.2)	
CTH	MBG8560530.1	K01758	Cystathionine γ-lyase	
CBS	MBG8560531.1	K01697	Cystathionine β-lyase	
TST	MBG8560836.1	K01011	Thiosulfate/3-mercaptopyruvate sulfurtransferase	

Table 4. *Cont.*

Gene	Accession Number	KO Number	Gene Product	Activity
bfr	MBG8560256.1	K03594	Bacterioferritin (EC:1.16.3.1)	Siderophore biosynthesis
entD	MBG8562760.1	K02362	Enterobactin synthetase component D (EC:6.3.2.14 2.7.8.-)	
fiu	MBG8560699.1	K16090	Catecholate siderophore receptor	Siderophore uptake
tonB	MBG8561215.1	K03832	Periplasmic protein tonb	
exbB	MBG8561408.1	K03561	Biopolymer transport protein exbb	
exbD	MBG8558382.1	K03559	Biopolymer transport protein exbd	
fepA	MBG8559634.1	K19611	Ferric enterobactin receptor	
pvdF	MBG8561616.1	K06160	Putative pyoverdin transport system ATP-binding/permease protein	
trpC	MBG8557998.1	K01609	Indole-3-glycerol phosphate synthase (EC:4.1.1.48)	Synthesis of the phytohormone:
trpD	MBG8557999.1	K00766	Anthranilate phosphoribosyltransferase (EC:2.4.2.18)	indole acetic acid (IAA)
trpG	MBG8558000.1	K01658	Anthranilate synthase component II (EC:4.1.3.27)	
trpE	MBG8558001.1	K01657	Anthranilate synthase component I (EC:4.1.3.27)	
trpF	MBG8560957.1	K01817	Phosphoribosylanthranilate isomerase (EC:5.3.1.24)	
trpA	MBG8562725.1	K01695	Tryptophan synthase alpha chain (EC:4.2.1.20)	
trpB	MBG8562726.1	K01696	Tryptophan synthase beta chain (EC:4.2.1.20)	
ipdC	MBG8559993.1	K04103	Indolepyruvate decarboxylase (EC:4.1.1.74)	
aspC	MBG8558823.1	K00813	Aspartate aminotransferase (EC:2.6.1.1)	
aldA	MBG8559624.1	K07248	Lactaldehyde dehydrogenase/glycolaldehyde dehydrogenase (EC:1.2.1.22 1.2.1.21)	
aldB	MBG8560334.1	K00138	Aldehyde dehydrogenase (EC:1.2.1.-)	
iaaM	MBG8558038.1	K00466	Amine oxidase	
acdS	MBG8559878.1	K01505	1-aminocyclopropane-1-carboxylate deaminase (EC:3.5.99.7)	Ethylene modulation
dcyD	MBG8561384.1	K05396	D-cysteine desulfhydrase (EC:4.4.1.15)	

Phosphorus is another essential nutrient for plants; however, a large proportion exists in an insoluble form and is thus unavailable for plants. Some soil bacteria play important roles in regulating P availability. This process is mainly mediated by enzymes involved in (1) inorganic P solubilization and organic P mineralization, (2) P uptake and transport, and (3) P starvation response regulation encoded by three corresponding groups of genes [34]. Genome analysis of the ZCR6 strain revealed the presence of genes from all three groups.

The first group contains the *gcd* gene coding for the quinoprotein glucose dehydrogenase (PQQGDH) and the *pqqABCDE* gene cluster necessary for pyrroloquinoline quinone (PQQ) cofactor biosynthesis (Table 4). PQQGDH is an enzyme that is responsible for the biosynthesis of gluconic acid (GA) in the direct oxidation pathway of glucose. The synthesis and secretion of GA is the major mechanism for the solubilization of mineral phosphate [26]. For the ZCR6 strain, P solubilization activity was also confirmed as a halo zone (6.5 mm diameter) on NBRIP agar plates containing an insoluble source of P (Table 1). Additionally, in the genome of ZCR6, the presence of the *ppa* and *ppx-gppA* genes, encoding inorganic pyrophosphatase and exopolyphosphatase, respectively, was detected. Inorganic pyrophosphatase catalyzes the hydrolysis of inorganic pyrophosphate PPi to inorganic phosphate Pi [35], while exopolyphosphatase catalyzes the hydrolysis of the terminal residues of inorganic polyphosphates (polyPs) to Pi [36].

The uptake of phosphate by bacteria occurs via two systems: the low-affinity, constitutively expressed Pit system and the high-affinity, phosphate-starvation-induced Pst

system [37]. In the genome of ZCR6, the presence of genes coding for both P uptake and transport systems (*pit* and *pstSCAB*) was reported (Table 4). These systems enable bacteria to assimilate inorganic P under P-rich and P-low conditions [22,38] and have also been described for many environmental strains, e.g., *Pseudomonas psychrotolerans* CS51, *Rhodococcus erythropolis* PR4, *Nocardioides sp.* JS614, *Catenulispora acidiphila* ID 139908^T, and *Frankia* sp. ACN14a [22,39–42].

The third group of genes, including *phoB*, *phoR*, and *phoU*, detected in the genome of ZCR6, was involved in P starvation regulation (Table 4). These genes are components of the Pho regulon, a regulatory circuit involved in bacterial phosphate management. PhoR-PhoB is a two-component regulatory system responsible for detecting and responding to changes in the P concentration in the environment, e.g., when phosphate becomes limited [43]. In this case, PhoR is stimulated to autophosphorylate and then transfer phosphoryl groups to PhoB. Phosphorylated PhoB undergoes a conformational change, allowing it to bind conserved DNA sequences called *pho* boxes in certain promoters, leading to increased transcription of genes, many of which help cells cope with decreased extracellular phosphate levels, e.g., genes involved in P uptake and transport (*pst*). In turn, the precise function of PhoU remains uncertain, and it is speculated that it may function as a negative regulator of the Pho regulon [44].

Sulfur, an essential macroelement required for plant growth, development, and response to environmental changes, is increasingly becoming limiting to plants [45]. Over 95% of the sulfur in soil is organically bound largely in one of two major forms—sulfate esters and sulfonates. These organic forms are not directly available to plants, which rely upon microbes in the rhizosphere for organo-S mobilization [46]. In the genome of the ZCR6 strain, the presence of genes encoding enzymes that are responsible for splitting the O-S bond in sulfate esters (arylsulfatase) and involved in the mobilization of SO_4 from sulfonates ($FMNH_2$-dependent monooxygenase enzyme complex, *ssu* gene cluster) was observed (Table 4). The metabolism of sulfur in the ZCR6 strain also involves the assimilation of inorganic sulfate.

Genome analysis revealed the presence of the *cysP*, *cysU*, *cysW*, and *cysA* genes encoding an ATP-binding cassette (ABC) transporter that includes periplasmic binding proteins (Table 4). These genes may be involved in the transportation of thiosulfate or inorganic sulfate to cells, as reported in the plant-growth-promoting *Sphingomonas* sp. LK11 *Pseudomonas* sp. UW4, *Cronobacter muytjensii* JZ38, and *Pseudomonas psychrotolerans* CS51 strains [22,26,28,47]. Additionally, genes encoding the sulfite reductase (NADPH) hemoprotein beta-component (*cysI*), the sulfite reductase (NADPH) flavoprotein alpha-component (*cysJ*), cystathionine γ-lyase (*CTH*), cystathionine β-lyase (*CBS*), and thiosulfate/3-mercaptopyruvate sulfurtransferase (*TST*) (Table 4), which are known for hydrogen sulfide (H_2S) production [47], were found. H_2S, at low concentrations, was revealed to be an important molecule produced by PGPB with a beneficial role in modulating plant growth and development, including seed germination, root organogenesis, stomatal closure, plant maturation, and flower senescence [48]. Additionally, H_2S improves the tolerance of plants to pathogens, osmotic stress, salt stress, heat shock, and heavy metal stresses [48], and the production of H_2S is the other mechanism of phosphate solubilization [49]

Iron (Fe) is an essential micronutrient for plants and microorganisms and is involved in various important biological processes, such as DNA synthesis, respiration, photosynthesis, and chlorophyll biosynthesis. Fe is generally present in soils in high quantities; however, its bioavailability in neutral pH and aerobic environments, in which iron is predominantly found in the Fe^{3+} form, is extremely low and, thus, is insufficient for organisms [50]. Bacteria can overcome iron limitation by producing siderophores, low-molecular mass molecules with strong affinity for chelating Fe^{3+}. A positive reaction for siderophore production was observed for the ZCR6 strain and observed as orange zones around the colonies (Table 1). In the genome of the ZCR6 strain, genes related to the biosynthesis of enterobactin (*entD*), bacterioferritin (*bfr*), and pyoverdine (*pvd*) were detected (Table 4). In addition, biosynthetic clusters of nonribosomal peptide synthetase (NRPS) engaged in pyoverdine

synthesis were identified using antiSMASH analysis (Table S2). In gram-negative bacteria, Fe-siderophore complexes are transported into the periplasm with the assistance of special receptor proteins called TonB-dependent receptors (TBDRs) [51]. The presence of the *tonB* gene encoding periplasmic protein, which provides the energy required for the translocation of siderophore–iron complexes across the bacterial outer membrane, along with the *fiu, exbB, exbD, fepA,* and *pvdF* genes encoding proteins involved in Fe-siderophore transport, was also detected in the ZCR6 genome (Table 4). Bacterial siderophores that can be efficiently used by plants have several functions in the rhizosphere [52–54]. Apart from increasing iron availability and thereby stimulating plant growth, siderophores can form stable complexes with other metals, such as Al, Cd, Cu, Pb, and Zn, and thus, can enhance their bioavailability. The resulting metal uptake by the plants caused by bacterial siderophores might enhance the effectiveness of the phytoremediation process [55].

2.4.2. Synthesis of the Phytohormone Indole3-Acetic Acid (IAA)

The ability of rhizospheric bacteria to promote plant growth is largely due to the production of auxin phytohormones, such as indole-3-acetic acid (IAA). IAA improves plant growth by stimulating root growth through cell proliferation and tissue expansion, as well as vascular bundle and nodule formation. Moreover, IAA plays a direct role in improving plant growth under stressful conditions; for example, it may prevent the deleterious effects of heavy metals [5]. It was found that bacterial IAA can slacken the cell walls of plants and, in this way, increase the amount of root exudates. These exudates control the higher metal concentration by chelating them in the rhizosphere and preventing them from entering the plant cellular pathways [56]. It has been reported that over 80% of bacteria isolated from the rhizosphere are capable of synthesizing IAA [57,58]. This feature was also quantitatively estimated for the ZCR6 strain. The studied strain released approximately 3.6 mg IAA mL^{-1} of medium (Table 1) and was classified as a low IAA producer. The main precursor for IAA biosynthesis in bacteria is L-tryptophan. Starting with tryptophan, different pathways have been reported for the synthesis of IAA; those that are more frequently described include (1) indole-3-pyruvate, (2) tryptamine, and (3) indole-3-acetamide. Genomic analysis of the ZCR6 strain revealed the presence of tryptophan (Trp) biosynthesis genes (*trpABCDE*) along with IAA biosynthesis genes involved in the indole-3-pyruvate pathway (*aspC, aldA, aldB,* and *ipdC*) (Table 4). In this pathway, indole-3-acetaldehyde is converted from indole-3-pyruvate by indolepyruvate decarboxylase (IpdC). In addition, the ZCR6 strain carried the *iaaM* gene encoding tryptophan-2-monooxygenase (IaaM), which oxidizes tryptophan to indole-3-acetamide, but the *iaaH* gene encoding indoleacetamide hydrolase (IaaH) was not found.

2.4.3. Ethylene Modulation

One of the mechanisms of plant growth promotion under various environmental stress conditions, such as the presence of organic and inorganic compounds, is the synthesis of 1-aminocyclo-propane-1-carboxylate (ACC) deaminase (ACCD), which is involved in lowering the level of ethylene. Ethylene is a phytohormone that controls the growth and maturation of plants. At low concentrations, ethylene participates in the regulation of plant growth and various metabolic processes; however, under stress conditions, plant ethylene levels increase significantly, adversely affecting the root growth and metabolism of the whole plant and leading to accelerated aging. In the genome of the ZCR6 strain, the *acdS* and *dcyD* genes, encoding ACCD and its homolog D-cysteine desulfhydrase, respectively, were detected (Table 4). Both enzymes are involved in hydrolyzing ACC, an immediate precursor of ethylene, to ammonia and α-ketobutyrate [59,60]. Consequently, the level of ACC in plant tissues is reduced, which results in a decreased level of endogenous ethylene, facilitating plant growth. In this relationship, the bacterium also benefits by utilizing the products of the reaction—nitrogen and carbon sources [61]. Biochemical characterization of the ZCR6 strain showed very high ACC deaminase activity (297 nmol α-ketobutyrate mg^{-1} h^{-1}) (Table 1), which is a sufficient value to support the growth of plants in polluted

soils. It was found that even a lower level of ACCD activity, approximately 20 nmol α-ketobutyrate mg^{-1} h^{-1}, is sufficient to support the growth of plants in harsh environmental conditions [62]. Hong et al. [63] demonstrated a positive effect of inoculation of a rhizobacterium strain, *Gordonia* sp. S2RP-17, on the phytodegradation of diesel-contaminated soil by *Z. mays* and found a positive correlation between hydrocarbon degradation and ACC deaminase activity. Additionally, in another study, Grobelak et al. [64] demonstrated that bacteria mainly belonging to the genera *Bacillus* and *Pseudomonas* had the highest ACC deaminase activity in environments contaminated with multiple heavy metals.

Except for the abovementioned PGP mechanisms, the ZCR6 strain degraded carboxymethylcellulose (CMC) (Table 1), which indicates its ability to produce cellulase, the enzyme that plays a crucial role during the colonization of interior tissues of plants [65]. It is worth emphasizing that the ability of rhizospheric bacteria to colonize plant interiors appears to be important for establishing close interactions with plants as endophytes, especially in contaminated environments [1]. The presence of this feature indicates the potential of the strain for the colonization of plant tissues and subsequent activity as an endophyte. In this case, endophytic bacteria can protect plants against diseases (e.g., via antibiotic synthesis) and directly influence the growth of plants [66].

2.5. Heavy Metal Resistance

Bacteria have developed a variety of resistance mechanisms to counteract heavy metal stresses. These mechanisms include the formation and sequestration of metal, its reduction to a less toxic form, and the direct efflux of metal out of the cell [67]. It is worth noting that the beneficial effects exhibited by the metal-resistant bacteria present in the rhizosphere might have significant potential to improve phytoextraction in metal-contaminated soils [68]. In addition to the ability of the ZCR6 strain to promote plant growth, the strain was able to overcome the toxic effects of heavy metals. Genomic analysis of the ZCR6 strain revealed the presence of a number of genes responsible for the detoxification and translocation of various heavy metals, such as Cd, Co, Zn, Cu, As, Cr, and Hg (Table 5). Furthermore, the resistance of the tested strain to Cd, Zn, and Cu was confirmed in minimal inhibitory concentration tests. The MIC values for Cd, Zn, and Cu in mineral medium reached 5, 15, and 10 mM metal, respectively. Interestingly, the ZCR6 strain was able to grow in higher concentrations of cadmium than well-known *P. putida* KNP9 (2.5 mM) [67].

Table 5. Genes potentially involved in metal resistance in the ZCR6 genome.

Gene	Accession Number	KO Numbers	Gene Product	Metal Resistance
czcA	MBG8562084.1	K15726	Cobalt-zinc-cadmium resistance protein czca	Cobalt/zinc/cadmium resistance
czcB	MBG8562085.1	K15727	Membrane fusion protein. Cobalt-zinc-cadmium efflux system	
czcC	MBG8562086.1	K15725	Outer membrane protein. Cobalt-zinc-cadmium efflux system	
copB	MBG8561457.1	K01533	P-type Cu^{2+} transporter (EC:7.2.2.9)	Cooper resistance
copA	MBG8562586.1	K17686	P-type Cu^{+} transporter (EC:7.2.2.8)	
cusR	MBG8559773.1	K07665	Two-component system. Ompr family. Copper resistance phosphate regulon response regulator cusr	
cusS	MBG8559774.1	K07644	Two-component system. Ompr family. Heavy metal sensor histidine kinase cuss (EC:2.7.13.3)	
cueR	MBG8562587.1	K19591	Merr family transcriptional regulator. Copper efflux regulator	

Table 5. *Cont.*

Gene	Accession Number	KO Numbers	Gene Product	Metal Resistance
arsR	MBG8562772.1	K03892	Arsr family transcriptional regulator. Arsenate/arsenite/antimonite-responsive transcriptional repressor	Arsenate resistance
arsB	MBG8559938.1	K03893	Arsenical pump membrane protein	
arsC	MBG8559939.1	K03741	Arsenate reductase (thioredoxin) (EC:1.20.4.4)	
arsC	MBG8562772.1	K00537	Arsenate reductase (glutaredoxin) (EC:1.20.4.1)	
arsH	MBG8559940.1	K11811	Arsenical resistance protein arsh	
chrA	MBG8559121.1	K07240	Chromate transporter	Chromium resistance
chrR	MBG8561757.1	K19784	Chromate reductase. Nad(p)h dehydrogenase (quinone)	
oprM	MBG8560149.1	K18139	Outer membrane protein. Efflux system	Multidrug resistance
acrB	MBG8560150.1	K18138	Multidrug efflux pump	
acrA	MBG8560151.1	K03585	Membrane fusion protein. Multidrug efflux system	
acrR	MBG8560152.1	K03577	Tetr/acrr family transcriptional regulator. Acrab operon repressor	
merE	MBG8560549.1	K00549	5-methyltetrahydropteroyltriglutamate–homocysteine methyltransferase (EC:2.1.1.14)	Mercury resistance

2.5.1. Cobalt/Zinc/Cadmium Resistance

In the genome of the ZCR6 strain, the presence of a *czc* operon comprising three structural genes, *czcC, czcB,* and *czcA* (Table 5), was found. Proteins encoded by the *czc* operon constitute a branch of metal-transporting resistance-nodulation-division-type (RND-type) efflux systems, corresponding to the first layer of metal resistance in bacteria [69]. The RND family plays an important role in the heavy metal resistance of gram-negative bacteria. These pumps function as a tripartite complex composed of the inner membrane and the periplasmic and outer membrane components [70]. In the CzcCBA efflux system, CzcC is a cell wall "outer" membrane protein, CzcA is an "inner" plasma membrane transport protein, and CzcB is a membrane fusion protein functioning as a dimer. The CzcCBA efflux pump functions to transport divalent cation/proton antiporters. This efflux pump is responsible for the detoxification of Zn^{2+}, Co^{2+}, and Cd^{2+} [71].

2.5.2. Copper/Arsenate/Chromium/Mercury Resistance

Furthermore, the ZCR6 genome also carried copper resistance genes—*copA, copB, cusR, cusS*, and *cueR* (Table 5). CopA and CopB are P-type Cu^+-ATPases responsible for transporting monovalent Cu from the cytoplasm, which is coupled to ATP hydrolysis [72]. Such Cu transporters function in many gram-negative bacteria, e.g., *Pseudomonas aeruginosa* [73], *Vibrio cholerae* [74], and *Salmonella enterica* sv. *typhimurium* [75]. CusRS is a two-component, signal transduction system that is responsive to copper ions and activates the expression of the *cus*CFBA operon. In turn, CusCFBA is involved in periplasmic copper detoxification [76]; however, the genome of the ZCR6 strain lacks this system. In addition, genome analysis of the ZCR6 strain revealed the presence of the *cueR* gene encoding CueR, which regulates the expression of the P-type Cu^+-ATPase [74].

Moreover, the presence of the *chrA* gene encoding a chromate transporter that acts as an efflux pump [77] and the *chrR* gene encoding chromate reductase that catalyzes a full reduction of Cr(VI) to Cr(III) [78] in the ZCR6 genome indicated a high degree of chromium (VI) resistance. Additionally, the arsenate resistance *arsRBC* system (Table 5) encodes ArsR, a transcriptional regulator; ArsB, an integral membrane protein that extrudes arsenite from the cell cytoplasm; and ArsC, an arsenate reductase able to transform arsenate to arsenite prior to extrusion of this metalloid [79]. ArsC enzymes use thioredoxin or glutaredoxin as electron sources; however, in the genome of the ZCR6 strain, the presence of both

homologs has been reported. Additionally, the genome of ZCR6 carried the *arsH* gene-encoded ArsH protein, which was demonstrated to be an organoarsenical oxidase enzyme conferring resistance to methyl As(III) derivatives in *Pseudomonas putida* and *Sinorhizobium meliloti* [80]. It is also worth emphasizing that the genome of the ZCR6 strain carrying the *merE* gene encodes a broad mercury transporter that mediates the transport of both Hg^{2+} and $CH_3Hg(I)$ across bacterial membranes [81].

2.5.3. Multidrug Resistance

In the genome of the ZCR6 strain, the presence of the *acrA, acrB*, and *oprM* genes encoding the AcrAB-OprM efflux system was detected (Table 5). This tripartite efflux system is composed of an inner membrane RND pump (AcrB), an outer membrane channel protein (OprM), and a periplasmic accessory protein (AcrA), and it was suggested to be responsible for multidrug resistance in gram-negative bacteria [82].

2.6. Exopolysaccharide (EPS) Production

The secretion of exopolysaccharides (EPS) by bacteria is a physiological process that is activated under a multitude of different environmental circumstances. The roles of these biopolymers includes basic functions such as maintaining the structural integrity of the cell envelope and enabling interactions within bacterial communities and between bacteria and eukaryotes [83]. The secretion of EPS by bacteria is also one of the most common mechanisms to protect the cell from the impact of adverse/harsh environmental conditions, such as starvation, pH, temperature, dehydration, or toxicity of heavy metals [84–86]. It is worth emphasizing that the genome of the ZCR6 strain carried the operons *bcs* and *alg*, involved in the biosynthesis of cellulose and alginate, respectively (Table 6). Due to the presence of various reactive groups on the polymer chains, biopolymers (including alginate and cellulose) or polymer-producing bacteria are considered to be the most attractive bioadsorbents, as they possess high selectivity and reactivity toward heavy metal ions and are recommended for the clean-up of heavy-metal-contaminated environments [87]. For example, a significant absorption capacity for Cd^{2+} or for both Cd^{2+} and Cu^{2+} was observed for *Pseudomonas* sp. strains 375 and DC-B3, respectively [88,89], indicating their potential to be used as low-cost, eco-friendly, and effective treatments for the bioremediation of heavy-metal-contaminated environments.

Table 6. Genes involved in exopolysaccharides production.

Gene	Accession Number	KO Numbers	Gene Product	Activity
bcsA	MBG8561468.1	K00694	Cellulose synthase (UDP-forming) (EC:2.4.1.12)	Exopolysaccharides biosynthesis
bcsB	MBG8561469.1	K20541	Cellulose synthase operon protein B	
bcsZ	MBG8561470.1	K20542	Endoglucanase (EC:3.2.1.4)	
bcsC	MBG8561471.1	K20543	Cellulose synthase operon protein C	
algF	MBG8561473.1	K19296	Alginate O-acetyltransferase complex protein algf	
algI	MBG8561474.1	K19294	Alginate O-acetyltransferase complex protein algi	
algJ	MBG8561475.1	K19295	Alginate O-acetyltransferase complex protein algj	
algB	MBG8562662.1	K11384	Two-component system. Ntrc family. Response regulator algb	
algA	MBG8559808.1	K16011	Mannose-1-phosphate guanylyltransferase/mannose-6-phosphate isomerase (EC:2.7.7.13 5.3.1.8)	
algL	MBG8560007.1	K01729	Poly(beta-D-mannuronate) lyase (EC:4.2.2.3)	
algX	MBG8560008.1	K19293	Alginate biosynthesis protein algx	
algG	MBG8560009.1	K01795	Mannuronan 5-epimerase (EC:5.1.3.37)	
algE	MBG8560010.1	K16081	Alginate production protein	
algK	MBG8560011.1	K19292	Alginate biosynthesis protein algk	

Table 6. *Cont.*

Gene	Accession Number	KO Numbers	Gene Product	Activity
alg44	MBG8560012.1	K19291	Mannuronan synthase (EC:2.4.1.33)	
alg8	MBG8560013.1	K19290	Mannuronan synthase (EC:2.4.1.33)	
algD	MBG8560014.1	K00066	GDP-mannose 6-dehydrogenase (EC:1.1.1.132)	
algH	MBG8561216.1	K07735	Putative transcriptional regulator	
algR	MBG8558298.1	K08083	Two-component system. Lyttr family. Response regulator algr	

2.7. Response to Oxidative Stress

It has been observed that rhizosphere bacteria are exposed to high levels of reactive oxygen species (ROS) that are formed along the plant root surface during the reaction of redox-active plant secondary metabolites, such as phenols, quinones, flavins, and phenazines, with molecular oxygen [90]. Additionally, upon contact with bacteria, one of the plant defense reactions is the production of ROS, nitric oxide and phytoalexins; thus, rhizosphere bacteria must survive in a highly oxidative environment during the colonization of plant tissues. Moreover, the degradation of aromatic compounds leads to the generation of ROS such as H_2O_2, OH^-, and O_2. Furthermore, heavy metal ions have been reported to promote increased formation of ROS [26,91] As part of adaptation, bacteria employ various enzymes, including catalases, peroxidases, and superoxide dismutases, for defense against reactive oxygen species (ROS). In the genome of ZCR6, we found a wide variety of enzymes that help to cope with oxidative stress (Table 7). Genome analysis of the ZCR6 strain revealed genes encoding enzymes such as hydrogen peroxide catalases (*katE* and *katG*), superoxide dismutases (*sod2*), glutathione S-transferases (*GST*), gamma-glutamyltranspeptidase/glutathione hydrolase (*ggt*), glutathione peroxidase (*gpx*), and glutathione reductase (*gor*). It is also worth emphasizing that the genome of the ZCR6 strain carried the *oxyR* gene, which encodes the hydrogen peroxide sensor OxyR activating the expression of a regulon of hydrogen peroxide-inducible genes. The presence of the abovementioned genes suggests that ZCR6 possesses the potential to overcome oxidative stress, which was also confirmed by phenotypic assays.

Table 7. Genes potentially involved in response to oxidative stress in the ZCR6 genome.

Gene	Accession Number	KO Numbers	Gene Product	Activity
katE	MBG8562679.1	K03781	Catalase (EC:1.11.1.6)	Oxidative stress response
katG	MBG8559566.1	K03782	Catalase-peroxidase (EC:1.11.1.21)	
sod2	MBG8560099.1	K04564	SOD2; superoxide dismutase. Fe-Mn family (EC:1.15.1.1)	
ggt	MBG8558271.1	K00681	Gamma-glutamyltranspeptidase/glutathione hydrolase (EC:2.3.2.2 3.4.19.13)	
gst	MBG8558300.1	K00799	Glutathione S-transferase (EC:2.5.1.18)	
gpx	MBG8560587.1	K00432	Glutathione peroxidase (EC:1.11.1.9)	
gsr	MBG8561128.1	K00383	GSR; glutathione reductase (NADPH) (EC:1.8.1.7)	
oxyR	MBG8558139.1	K04761	Lysr family transcriptional regulator. Hydrogen peroxide-inducible gene activator	

2.8. Organic Compound Degradation and Biosurfactant Production

Numerous studies have shown that bacteria belonging to the genus *Pseudomonas* are known for their ability to degrade aliphatic and/or aromatic organic compounds [4,92]. For example, Muriel-Millán et al. [93] reported that the *P. aeruginosa* strain GOM1 degraded 96% of the aliphatic fraction (C12–C38) of crude oil during a 30-day incubation period, exhibiting high activity against long-chain alkanes and expressing alkane hydroxylases. In another study, Mahjoubi et al. [94] described that *Pseudomonas* sp. BUN14 could grow on

and utilize various aromatic hydrocarbons, including pyrene, naphthalene, phenanthrene, carbazole, dibenzofuran, dibenzothiophene, biphenyl, pristane, fluoranthene, crude oil, octadecane, and tetradecane, as sole carbon and energy sources. It is worth noting that the effectiveness of phytoremediation supported by bacteria depends mainly on the activity of microorganisms carrying catabolic genes [95,96]. To investigate the potential of the ZCR6 strain to degrade both aliphatic and aromatic hydrocarbons, we explored its genome in search of genes related to the corresponding degradation pathways. The ZCR6 genome contains crucial genes involved in the degradation of these compounds (Table 8), which emphasizes that this strain is an excellent candidate for bioremediation.

Table 8. Genes involved in organic compounds' degradation.

Gene	Accession Number	KO Numbers	Gene Product	Activity
ladA	MBG8560652.1	K20938	long-chain alkane monooxygenase (EC:1.14.14.28)	Aliphatic compounds' degradation
pcaG	MBG8562545.1	K00448	Protocatechuate 3.4-dioxygenase. Alpha subunit (EC:1.13.11.3)	
pcaH	MBG8562546.1	K00449	Protocatechuate 3.4-dioxygenase. Beta subunit (EC:1.13.11.3)	
pcaQ	MBG8560766.1	K02623	Lysr family transcriptional regulator. Pca operon transcriptional activator	
pcaC	MBG8560139.1	K01607	4-carboxymuconolactone decarboxylase (EC:4.1.1.44)	
pcaD	MBG8560138.1	K01055	3-oxoadipate enol-lactonase (EC:3.1.1.24)	
pcaR	MBG8560131.1	K02624	Iclr family transcriptional regulator. Pca regulon regulatory protein	
pcaK	MBG8560132.1	K08195	MFS transporter. AAHS family. 4-hydroxybenzoate transporter	
pcaF	MBG8560135.1	K07823	3-oxoadipyl-coa thiolase (EC:2.3.1.174)	
pcaT	MBG8560136.1	K02625	MFS transporter. MHS family. Dicarboxylic acid transporter pcat	
pcaB	MBG8560137.1	K01857	3-carboxy-cis.cis-muconate cycloisomerase (EC:5.5.1.2)	Aromatic compounds' degradation
hpaF	MBG8558716.1	K01826	5-carboxymethyl-2-hydroxymuconate isomerase (EC:5.3.3.10)	
hpaI	MBG8558890.1	K02510	4-hydroxy-2-oxoheptanedioate aldolase (EC:4.1.2.52)	
hpaH	MBG8558891.1	K02509	2-oxo-hept-3-ene-1.7-dioate hydratase (EC:4.2.1.-)	
hpaF	MBG8558893.1	K01826	5-carboxymethyl-2-hydroxymuconate isomerase (EC:5.3.3.10)	
hpaD	MBG8558894.1	K00455	3.4-dihydroxyphenylacetate 2.3-dioxygenase (EC:1.13.11.15)	
hpaE	MBG8558895.1	K00151	5-carboxymethyl-2-hydroxymuconic-semialdehyde dehydrogenase (EC:1.2.1.60)	
hpaG	MBG8558896.1	K05921	5-oxopent-3-ene-1.2.5-tricarboxylate decarboxylase/2-hydroxyhepta-2.4-diene-1.7-dioate isomerase (EC:4.1.1.68 5.3.3.-)	
hpaA	MBG8558898.1	K02508	Arac family transcriptional regulator. 4-hydroxyphenylacetate 3-monooxygenase operon regulatory protein	
paaF	MBG8559324.1	K01692	Enoyl-coa hydratase (EC:4.2.1.17)	
paaX	MBG8559346.1	K02616	Phenylacetic acid degradation operon negative regulatory protein	
paaY	MBG8559347.1	K02617	Phenylacetic acid degradation protein	
paaG	MBG8559349.1	K15866	2-(1.2-epoxy-1.2-dihydrophenyl)acetyl-coa isomerase (EC:5.3.3.18)	

Table 8. *Cont.*

Gene	Accession Number	KO Numbers	Gene Product	Activity
paaH	MBG8559350.1	K00074	3-hydroxybutyryl-coa dehydrogenase (EC:1.1.1.157)	
paaI	MBG8559351.1	K02614	Acyl-coa thioesterase (EC:3.1.2.-)	
paaK	MBG8559353.1	K01912	Phenylacetate-coa ligase (EC:6.2.1.30)	
paaA	MBG8559354.1	K02609	Ring-1.2-phenylacetyl-coa epoxidase subunit paaa (EC:1.14.13.149)	
paaB	MBG8559355.1	K02610	Ring-1.2-phenylacetyl-coa epoxidase subunit paab	
paaC	MBG8559356.1	K02611	Ring-1.2-phenylacetyl-coa epoxidase subunit paac (EC:1.14.13.149)	
paaD	MBG8559357.1	K02612	Ring-1.2-phenylacetyl-coa epoxidase subunit paad	
paaE	MBG8559358.1	K02613	Ring-1.2-phenylacetyl-coa epoxidase subunit paae	
paaZ	MBG8559362.1	K02618	Oxepin-coa hydrolase/3-oxo-5.6-dehydrosuberyl-coa semialdehyde dehydrogenase (EC:3.3.2.12 1.2.1.91)	
etbAa;	MBG8559252.1	K14748	Ethylbenzene dioxygenase subunit alpha (EC:1.14.12.-)	
etbAb;	MBG8559253.1	K14749	Ethylbenzene dioxygenase subunit beta (EC:1.14.12.-)	

2.8.1. Degradation of Aliphatic Hydrocarbons

The genome of the ZCR6 strain carried *ladA*—a functional gene determining a novel type of alkane monooxygenase (LadA) (Table 8) that was originally detected in the genome of thermophilic *Geobacillus thermodenitrificans* NG80-2 [97]. LadA is a flavin-dependent long-chain alkane monooxygenase of the family of bacterial luciferases that utilizes a terminal oxidation pathway for the conversion of long-chain alkanes (C15 and longer, up to C36) to corresponding alcohols [98–100]. To the best of our knowledge, this is the first work that shows the presence of the *ladA* gene in the genome of the *Pseudomonas* genus. The ability of ZCR6 to degrade crude oil hydrocarbons was confirmed by measuring the amount of residual hydrocarbons in the culture medium during 4 weeks of cultivation. The fastest degradation rate was observed in the first week of cultivation—45.6% of the initial hydrocarbon content was degraded. In the following weeks, the rate of degradation was slower, and 76.52% of the initial hydrocarbon content was finally removed after four weeks of bacterial culture (Figure 5).

2.8.2. Degradation of Aromatic Hydrocarbons

Aromatic compounds are both common growth substrates for microorganisms and prominent environmental pollutants [101]. These structurally diverse compounds are independently converted into a small number of structurally simpler common intermediates, such as catechol and protocatechuate [102]. The β-ketoadipate pathway is present in many bacterial groups, including gram-positive and gram-negative bacteria, and is considered one of the most widely distributed sets of genes for the degradation of aromatic compounds in microbes. This central pathway is composed of two ortho-cleavage branches, one for degradation of protocatechuate (*pca* genes) and the other for degradation of catechol (*cat* genes) [103]. Both protocatechuate and catechol are central metabolites derived from the oxygenation of different phenolic compounds, lignin monomers and polyaromatic hydrocarbons [104]. The final products of both pathways are acetyl-CoA and succinyl CoA [105]. It is worth noting that the protocatechuate branch of the β-ketoadipate pathway is ubiquitous in completely sequenced *Pseudomonas* genomes [28], emphasizing the importance of aromatic compound catabolism by these bacteria. Genome analysis of

the ZCR6 strain revealed the presence of the *pca* cluster encoding enzymes engaged in protocatechuate catabolism but a lack of *cat* clusters. Furthermore, in the genome of the ZCR6 strain, the *hpa* genes of the homoprotocatechuate catabolic pathway were identified (Table 8). Homoprotocatechuate (3,4-dihydroxyphenylacetic acid HPC) is meta-cleaved by an HPC 2,3-dioxygenase encoded by the *hpaD* gene. The product 5-carboxymethyl-2-hydroxymuconic semialdehyde (CHMS) is then converted to 5-carboxymethyl-2-hydroxy-muconic acid (CHM) and subsequently degraded by the *hpaF, hpaG, hpaH* and *hpaI* gene products into Krebs cycle intermediates [106]. The *paa* cluster encoding enzymes involved in the phenylacetyl-CoA pathway was also present in the genome of the ZCR6 strain (Table 8). This pathway constitutes a catabolon through which many other structurally related compounds, such as phenylethylamine, phenylethanol, styrene, tropate, and n-phenylalkanoates with an even number of carbon atoms, are funneled [103]. Moreover, the ZCR6 strain contained genes for catabolism of ethylbenzene (*etbAa and etbAb*) and naphthalene (*nagZ*).
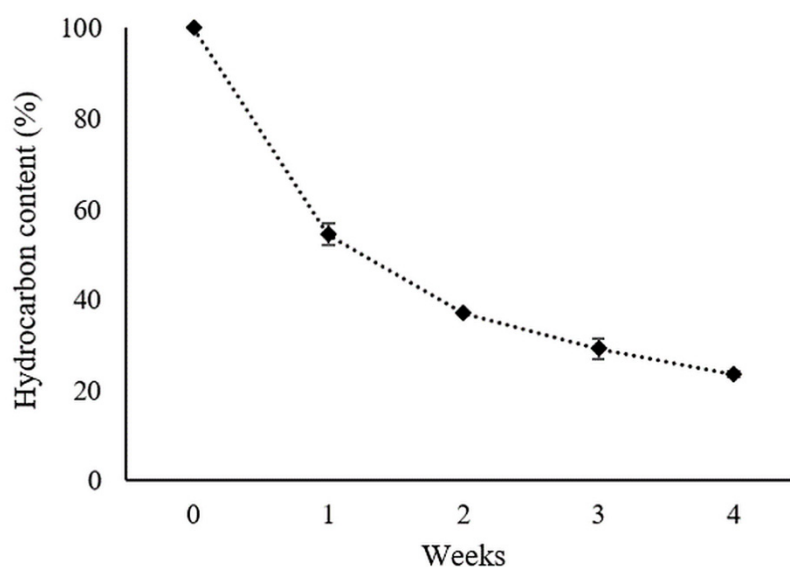
Figure 5. Degradation of hydrocarbons by the ZCR6 strain (mean ± SD, n D 3).

During the biodegradation of hydrocarbons, the bioavailability of these compounds is considered a key limiting factor due to their low aqueous solubility and high hydrophobicity. To enhance the bioavailability of hydrocarbons, microorganisms produce biosurfactants [107,108]. The biosurfactants produced by bacteria can also contribute to inhibiting the growth of phytopathogens, help colonize plant tissues and improve bacterial motility [109]. In this study, the ZCR6 strain produced a surface-active compound, which showed a positive result for the oil-spreading test and exhibited emulsification activities against *p*-xylene (E24 = 71.43% ± 1.43), diesel oil (E24 = 14.71% ± 0.29) and *n*-hexadecane (E24 = 25.71% ± 0.57) (Table 1). These results suggest that the ability of ZCR6 to degrade crude oil may be linked with the production of biosurfactants. For example, Cheng et al. [110] reported that *Pseudomonas aeruginosa* ZS1 isolated from petroleum sludge produced a high level of rhamnolipid that effectively emulsified crude oil, accelerating its uptake and degradation. Literature data indicate that members of the genus *Pseudomonas* possess robust metabolic machinery with the inherent ability to produce multiple and diverse secondary metabolites, including biosurfactants [111]. Genome mining by antiSMASH 5.0 resulted in the prediction of seven gene clusters associated with secondary metabolite biosynthesis (Table S2). Many of the biosynthetic gene clusters (BGCs) are predicted to encode nonribosomal peptide synthetases (NRPSs), which produce lipopeptide (LP) and biosurfactants such as rhizomide B, viscosin, gacamide A, putisolvin, orfamide B, and anikasin. The structures of these secondary metabolites were predicted using PubChem

and are presented in Supplementary Figure S2. It is worth noting that LPs and rhamno-lipids have been successfully used to enhance oil recovery in extreme environmental conditions [112]. In addition, bacteria use LPs for the chelation of heavy metals in a similar way to siderophores and incorporate them into their metabolism as micronutrients [113].

3. Materials and Methods

3.1. Isolation of Hydrocarbon-Degrading and Metal-Resistant Bacterial Strains

The hydrocarbon-degrading and metal-resistant strains were isolated from the rhizo-sphere of *Zea mays* growing in soil co-contaminated with hydrocarbons and heavy metals taken in the vicinity of the Coke Plant "Jadwiga" in Zabrze (Zabrze, Upper Silesia, Poland) using an enrichment technique. Ten grams of soil was initially suspended in 90 mL of an M9 mineral salt medium (Na_2HPO_4 6 g, KH_2PO_4 3 g, NaCl 0.5 g, NH_4Cl 1 g, $MgSO_4·7H_2O$ 0.24 g, and $CaCl_2$ 0.01 g per liter of deionized water) [114] supplemented with 1% (*v/v*) crude oil as a carbon and energy source and 3 mM zinc as $ZnSO_4$. The incubation was performed at 28 °C on a rotary shaker at 120 rpm for seven days. Continuous subculturing and shaking were carried out three times for enrichment. Next, a soil suspension was inoculated on M9 agar plates supplemented with 1% (*v/v*) crude oil and 3 mM $ZnSO_4$, and 26 morphologically different colonies were reinoculated on M9 plates supplemented with crude oil and Zn. Isolates were then studied for their plant-growth-promoting and surface-active activities.

3.2. Evaluation of Plant-Growth-Promoting Activities and Surface-Active Properties

The PGP abilities of the isolates were characterized by several biochemical tests. 1-Aminocyclopropane-1-carboxylic acid (ACC) deaminase activity was assayed as de-scribed by [115] and expressed in nmol of α-ketobutyrate mg^{-1} of protein h^{-1}. The protein concentration of microbial cell extracts was determined by Bradford method [116]. The cel-lulase activity was examined by the inoculation of the isolates on carboxymethyl cellulose agar plates as described by Pointing [117]. Siderophore secretion by the tested strain was detected by the Schwyn and Neilands method [118] using blue agar plates containing the dye Chrome azurol S (CAS). Orange zones around the colonies on the blue agar were con-sidered positive reactions for siderophore production. Indole acetic acid (IAA) production was determined according to the modified method of Bric et al. [119] using Salkowski's reagent. The IAA concentration in cultures was determined using a calibration curve of pure IAA (concentration range from 1 to 100 μg mL^{-1}) as the standard and the production of ammonia in peptone water according to Cappuccino and Sherman [120]. The phosphate solubilizing ability of the tested strain was determined on NBRIP agar medium. Bacteria were stabbed using a sterile needle. The halo and colony diameters were measured after 14 days of incubation at 28 °C. Halo size was calculated by subtracting the colony diameter from the total diameter [121]. The production of hydrogen cyanide was tested using the method described by Lorck [122].

The surface-active properties of the strains were analyzed using the oil-spreading test and by evaluating the emulsification capacity for *n*-hexadecane, *p*-xylene, and diesel oil (by calculating the value of the emulsification index (E24)) according to the protocols described by Pacwa-Płociniczak et al. [123]. Additionally, the ability of the strains to reduce surface tension was measured using the Krűss K20 force tensiometer according to the protocol described by Ptaszek et al. [124].

All experiments were performed in triplicate and had positive (*Enterobacter intermedius* MH8b) and negative (blank, without bacterial cultivation) controls.

Based on the results of the above tests, the most promising ZCR6 strain was chosen for further analysis.

3.3. Biochemical Characteristics and Cellular Fatty Acid Analysis of ZCR6 Strain

The ZCR6 strain was tested for the hydrolysis of starch using starch agar flooded with iodine [125] and for the hydrolysis of gelatin using nutrient gelatin agar flooded

with HgCl$_2$ (15%) in HCl (20%, *v/v*) [126]. The activity of dehydrogenase was tested by studying the utilization of hydrogen in the presence of methylene blue solution (1% *v/v*) [127], oxidase activity was tested on filter paper impregnated with tetramethyl-*p*-phenylenediamine [128], catalase activity was studied using broth agar flooded with H$_2$O$_2$ (3%, *v/v*) [126], urease activity was checked using nutrient broth containing urea and phenol red [129], arginine dihydrolase activity was tested using nutrient agar supplemented with L-arginine and phenol red [128], and nitrate reductase activity was tested using broth medium supplemented with KNO$_3$ and nitrite test reagents [126]. Additionally, pigment formation was tested on King A and King medium B [130].

Before fatty acid extraction, bacteria were grown according to the manufacturer's protocol on TSA agar medium at 28 °C and were reinoculated three times on fresh TSA medium to stabilize the fatty acid composition. Initially, fatty acids were released and saponified by the addition 1mL of reagent 1 (45 g NaOH, 150 mL methanol, 150 mL water) to the sample and incubation at 100 °C for 30 min with occasional vortexing. Next, free fatty acids were methylated by adding reagent 2 (325 mL 6 N HCl, methanol 275 mL) solution (2 mL) and incubated at 80 °C for 10 min. Phase separation was then carried out by the addition 1 mL of reagent 3 (1:1 mixture of n-hexane and methyl-tert butyl ether) with vigorous mixing by vortex for 30 s. After sufficient phase separation, the top organic phase was transferred to a new glass tube and washed with 3 mL of NaOH solution (10.8 g NaOH, 900 mL water). The top organic phase was again transferred to a new GC vial and analyzed according to the standard protocol of MIDI (Sherlock Microbial Identification System, version 6.0) and identified using the TSBA 6.21 database of the Microbial Identification System as described in [131].

3.4. DNA Extraction, Whole Genome Sequencing, and Assembly

A single colony of the ZCR6 strain taken from an M9 agar plate supplemented with crude oil and Zn was reinoculated into 30 mL of liquid M9 medium with 1% (vol/vol) crude oil and 3 mM Zn and incubated at 28 °C on a rotary shaker at 120 rpm for 48 h. Genomic DNA was extracted using the GeneMatrix Bacterial and Yeast Genomic Purification Kit according to the manufacturer's instructions (EURx®, Gdańsk, Poland). Genomic libraries were constructed using the NEBNext® DNA Library Prep Master Mix Set for Illumina® and sequenced using the Illumina MiSeq platform with 2 × 250 bp paired-end reads (Illumina, San Diego, SD, USA). The primer sequences were trimmed out of the reads using Cutadapt 1.16 (phred score cutoff: 20; maximum trimming error rate: 0.1; minimum required adapter overlap: 3 bp). Reads were assembled using SPAdes 3.11.1 (to generate contigs, default parameters were used; error correction and Kmer sizes were set to auto). Genome sequences were deposited in the GenBank database under BioProject accession number PRJNA681194 under accession number JADWSX000000000.

3.5. Genome Functional Annotation

Functional annotation of genes was performed using a multitude of tools and databases, such as the NCBI Prokaryotic Genome Annotation Pipeline (PGAP) (www.ncbi.nlm.nih.gov/genome/annotation_prok/, accessed on 1 December 2020), the eggNOG 5.0 orthology prediction pipeline (http:/eggnogdb.embl.de, accessed on 15 May 2020) [132], and the PATRIC tool v.3.6.9 (https://www.patricbrc.org, accessed on 15 May 2020) [133]. For annotation of gene function, genes were compared to the KEGG database (Functional Kyoto Encyclopedia of Genes and Genomes database) (http://www.genome.jp/kegg/, accessed on 15 May 2020) [134]. Functional and pathway analyses were also performed using the BlastKOALA web tool of KEGG (https://www.kegg.jp/blastkoala/, accessed on 15 May 2020) [134]. A subsequent annotation was performed using Rapid Annotations using a Subsystems Technology tool kit (RASTtk) found in PATRIC tool v.3.6.9. Functional analysis by Cluster of Orthologous Genes (COGs) was performed with the use of WebMGA (http://weizhong-lab.ucsd.edu/webMGA/server/cog/, accessed on 15 May 2021) [135]. Identification of gene clusters responsible for biosynthesis of secondary metabolites was per-

formed using antiSMASH 5.0 (https://antismash.secondarymetabolites.org, accessed on 15 May 2021) [136]. Prophage sequences were identified and annotated using PHAST [137]. The circular genome was generated with the PATRIC tool v.3.6.9. For genome functional annotation, all the default parameters were used for the analysis.

3.6. Phylogenetic Analysis

To check the taxonomic placement of the ZCR6 strain, the 16S rRNA gene was amplified with the universal bacterial primers 8F (5′ AGTTTGATCATCGCTCAG 3′) and 1492R (5′ GGTTACCTTGTTACGACTT 3′), targeting a fragment size of 1484 bp [107]. Next, the obtained sequence with a length of 1402 bp was compared with the EZBioCloud database. The phylogenetic analysis was performed based on the longest common fragment of the 16S rRNA gene sequences (1387 bp) selected from ClustalW alignment of ZCR6 strains and 13 type strains of other *Pseudomonas* species. Sequences of 16S rRNA fragments of type strains were obtained from GenBank. The analysis was performed using Mega X software with the maximum likelihood method and the Tamura-3-parameter model, assuming that a certain fraction of sites are evolutionarily invariable (+I) and 1000 bootstrap replicates [138,139]. The similarity of 16S rRNA sequences between tested and type strains was calculated using the average nucleotide identity (ANI) calculator (https://www.ezbiocloud.net/tools/ani, accessed on 12 September 2021) [140].

Detailed identification of the ZCR6 strain was obtained using multilocus sequence analysis (MLSA) of the partial sequences of 16S rRNA and two housekeeping genes (*gyrB and rpoD*) [20,138]. After alignment using ClustalW, the concatenated sequences (2563 bp for 16S rRNA-*gyrB-rpoD* genes) were compared with concatenated sequences of type strains obtained from GenBank (accession numbers of sequences are given in Supplementary Table S1). Phylogenetic analysis of the ZCR6 strain was performed using Mega X software with the maximum likelihood method with 1000 bootstrap replicates under the Tamura–Nei model using the discrete gamma distribution (+G) [138]. The similarity of concatenated gene sequences between tested and type strains was calculated using the ANI calculator. Additionally, using the TrueBac ID tool (truebacid.com, accessed on 16 November 2020), the isolate was identified based on the sequence of the entire genome [141]. The target genes were extracted from the entire genome using Geneious Prime software.

A tetra-correlation search (TCS), a feature of JSpeciesWS (http://jspecies.ribohost.com/jspeciesws, accessed on 15 May 2020) [142], allowed comparisons of the genome sequenced of the ZCR6 strain against the genomes from the reference database GenomesDB, providing a list of the most similar genomes based on their resulting tetranucleotide signature correlation index.

3.7. Hydrocarbon Degradation Analysis

The ability of the ZCR6 strain to degrade crude oil was studied in 0.1 LB (Luria Bertani) broth. Replicate flasks containing 500 mL of medium supplemented with crude oil at a 1% concentration (*v/v*) were prepared. The flasks were inoculated with 5 mL of one-week-old liquid culture of the ZCR6 strain. Non-inoculated flasks were prepared as controls. The cultures were grown aerobically at 28 °C for 4 weeks with constant shaking (120 rpm). To determine the amount of hydrocarbon degraded, the initial concentration of hydrocarbons and the residual hydrocarbon concentration after 4 weeks of incubation were determined.

The mineral oil content was estimated according to PN-EN ISO 9377-2. The quantitative determination of mineral oil (hydrocarbon) content after extraction was estimated by gas chromatography. The 0.1 LB medium with crude oil was extracted by mechanical shaking with an acetone/*n*-heptane mixture for 1 h at 120 rpm. The organic layer was separated and washed twice with water to remove acetone. The remaining *n*-heptane extract was dried using anhydrous Na_2SO_4. Polar compounds were removed by adsorption on Florisil®/Na_2SO_4 columns. An aliquot of the purified extract was analyzed by GC-FID. The total peak area in the range C_{10}-C_{40} was measured, and the amount of hydrocarbons in the sample was quantified against an external standard.

The total petroleum hydrocarbon (TPH) content was analyzed using a gas chromatograph (Agilent 7820A) equipped with a flame ionization detector and an Rxi-5ms capillary column (25 m × 0.2 mm ID × 0.33 μm); the injection volume was 1 μL, and hydrogen was used as the carrier gas (gas flow 2.1 mL minute^{-1}). The operation program was started with injector and detector temperatures of 300 °C. The oven temperature was initially programmed at 60 °C, held for 10 min, increased to 320 °C at 30 °C minute^{-1}, and then held for 10 min.

3.8. Minimal Inhibitory Concentration (MIC) Determination

The level of resistance to heavy metals of the ZCR6 strain was assessed by determination of the minimal inhibitory concentration (MIC) of Zn^{2+}, Cu^{2+}, Cd^{2+}, and Ni^{2+} ions as described by [143]. The MIC values were determined in triplicate in Tris minimal salt medium with glucose (Tris-MSM) (Tris base 1 g, glucose 5 g, NaCl 0.5 g, KCl 0.5 g, $MgSO_4·7H_2O$ 0.2 g, $(NH_4)_2SO_4$ 0.5 g, $CaCl_2$ 0.01, $FeSO_4·7H_2O$ 0.001 g per liter of deionized water with pH range of 7.0 ± 0.2.) [144]. The Tris-MSM medium was supplemented with increasing concentrations of the metals (0.5–20 mM). The inoculum was prepared by culturing the ZCR6 strain in LB medium at 28 °C on a rotary shaker at 120 rpm for 24 h. After incubation, the culture was centrifuged at 5000 rpm for 20 min, washed twice with sterile sodium chloride (0.9%), and resuspended in Tris-MSM medium. Media amended with different concentrations of heavy metals were inoculated with bacterial inoculum to obtain an optical density (OD) of 0.1 at 600 nm. As for the controls, medium with inoculum but without metal and medium amended with metals but without inoculum were prepared. Cultures were incubated at 28 °C on a rotary shaker at 120 rpm, and the OD was measured after 72 h. The MIC was defined as the lowest metal concentration at which bacterial growth was not observed.

4. Conclusions

In this study, we confirmed that the *P. qingdaonensis* ZCR6 strain isolated from the rhizosphere of maize exhibits potential for the bioremediation of sites co-contaminated with hydrocarbons and heavy metals using this plant. However, the potential contamination of plant biomass should be considered when conducting the phytoremediation experiments using crop plants, e.g., maize. On the other hand, in most cases, the seeds of plants are protected, and heavy metals are not accumulated in such structures; thus, their application is possible. Nevertheless, phytoremediation should be conducted under controlled conditions, and plant biomass cannot be used as food for animals and humans.

The examined strain shows the potential to promote plant growth through a wide range of mechanisms, such as the production of IAA, ACC deaminase, siderophores, ammonia and solubilization of phosphate. It is worth noting that these mechanisms can also affect the effectiveness of the bioremediation process. Additionally, sequencing of the ZCR6 strain genome provided important information about features that may be crucial for bioremediation. Notably, genetic analyses were linked with the outcomes of previously performed assays, expanding the understanding of genome–phenotype interplays. We identified the genes involved in the metabolism and degradation of xenobiotics. Furthermore, genome sequencing of ZCR6 opened up a number of opportunities to study the mechanisms involved in the production of secondary metabolites via PGP, including biosurfactants and metal resistance. We believe that our research provided substantial interesting data about a new *P. qingdaonensis* species. Complete characteristics of the ZCR6 strain are beneficial for fully understanding the mechanisms involved in the bioremediation of co-contaminated sites.

Supplementary Materials: The following supporting information can be downloaded at: https://www.mdpi.com/article/10.3390/ijms23010214/s1.

References

1. Germaine, K.J.; Keogh, E.; Ryan, D.; Dowling, D.N. Bacterial endophyte-mediated naphthalene phytoprotection and phytoremediation. *FEMS Microbiol. Lett.* **2009**, *296*, 226–234. [CrossRef] [PubMed]
2. Glick, B.R. Using soil bacteria to facilitate phytoremediation. *Biotechnol. Adv.* **2010**, *28*, 367–374. [CrossRef]
3. Afzal, M.; Khan, Q.M.; Sessitsch, A. Endophytic bacteria: Prospects and applications for the phytoremediation of organic pollutants. *Chemosphere* **2014**, *117*, 232–242. [CrossRef] [PubMed]
4. Khan, S.; Afzal, M.; Iqbal, S.; Khan, Q.M. Plant-bacteria partnerships for the remediation of hydrocarbon contaminated soils. *Chemosphere* **2013**, *90*, 1317–1332. [CrossRef] [PubMed]
5. Manoj, S.R.; Karthik, C.; Kadirvelu, K.; Arulselvi, P.I.; Shanmugasundaram, T.; Bruno, B.; Rajkumar, M. Understanding the molecular mechanisms for the enhanced phytoremediation of heavy metals through plant growth promoting rhizobacteria: A review. *J. Environ. Manag.* **2020**, *254*, 109779. [CrossRef]
6. Jeelani, N.; Yang, W.; Xu, L.; Qiao, Y.; An, S.; Leng, X. Phytoremediation potential of Acorus calamus in soils co-contaminated with cadmium and polycyclic aromatic hydrocarbons. *Sci. Rep.* **2017**, *7*, 8028. [CrossRef]
7. Bello-Akinosho, M.; Makofane, R.; Adeleke, R.; Thantsha, M.; Pillay, M.; Johannes Chirima, G. Potential of Polycyclic Aromatic Hydrocarbon-Degrading Bacterial Isolates to Contribute to Soil Fertility. *BioMed Res. Int.* **2016**, *2016*, 5798593. [CrossRef]
8. Das, K.; Abrol, S.; Verma, R.; Annapragada, H.; Katiyar, N.; Senthilkumar, M. Pseudomonas. *Benef. Microbes Agro-Ecol.* **2020**, 133–148. [CrossRef]
9. Sun, K.; Liu, J.; Gao, Y.; Li, J.; Gu, Y.; Wang, W. Isolation, plant colonization potential, and phenanthrene degradation performance of the endophytic bacterium *Pseudomonas* sp. Ph6-gfp. *Sci. Rep.* **2014**, *4*, 5462. [CrossRef]
10. Zhu, X.; Ni, X.; Waigi, M.G.; Liu, J.; Sun, K.; Gao, Y. Biodegradation of Mixed PAHs by PAH-Degrading Endophytic Bacteria. *Int. J. Environ. Res. Public Health* **2016**, *13*, 805. [CrossRef]
11. Wu, T.; Xu, J.; Xie, W.; Yao, Z.; Yang, H.; Sun, C.; Li, X. *Pseudomonas aeruginosa* L10: A hydrocarbon-degrading, biosurfactant-producing, and plant-growth-promoting endophytic bacterium isolated from a Reed (*Phragmites australis*). *Front. Microbiol.* **2018**, *9*, 1087. [CrossRef]
12. Khan, Z.; Roman, D.; Kintz, T.; Delas Alas, M.; Yap, R.; Doty, S. Degradation, Phytoprotection and Phytoremediation of Phenanthrene by Endophyte *Pseudomonas putida*, PD1. *Environ. Sci. Technol.* **2014**, *48*, 12221–12228. [CrossRef] [PubMed]
13. Germaine, K.J.; Liu, X.; Cabellos, G.G.; Hogan, J.P.; Ryan, D.; Dowling, D.N. Bacterial endophyte-enhanced phytoremediation of the organochlorine herbicide 2,4-dichlorophenoxyacetic acid. *FEMS Microbiol. Ecol.* **2006**, *57*, 302–310. [CrossRef] [PubMed]
14. Bakaeva, M.; Kuzina, E.; Vysotskaya, L.; Kudoyarova, G.; Arkhipova, T.; Rafikova, G.; Chetverikov, S.; Korshunova, T.; Chetverikova, D.; Loginov, O. Capacity of Pseudomonas Strains to Degrade Hydrocarbons, Produce Auxins and Maintain Plant Growth under Normal Conditions and in the Presence of Petroleum Contaminants. *Plants* **2020**, *9*, 379. [CrossRef]
15. Płociniczak, T.; Sinkkonen, A.; Romantschuk, M.; Piotrowska-Seget, Z. Characterization of Enterobacter intermedius MH8b and its use for the enhancement of heavy metals uptake by *Sinapis alba* L. *Appl. Soil Ecol.* **2013**, *63*, 1–7. [CrossRef]
16. Chellaiah, E.R. Cadmium (heavy metals) bioremediation by Pseudomonas aeruginosa: A minireview. *Appl. Water Sci.* **2018**, *8*, 154. [CrossRef]

17. Płociniczak, T.; Chodór, M.; Pacwa-Płociniczak, M.; Piotrowska-Seget, Z. Metal-tolerant endophytic bacteria associated with Silene vulgaris support the Cd and Zn phytoextraction in non-host plants. *Chemosphere* **2019**, *219*, 250–260. [CrossRef]

18. Das, D.; Baruah, R.; Sarma Roy, A.; Singh, A.K.; Deka Boruah, H.P.; Kalita, J.; Bora, T.C. Complete genome sequence analysis of Pseudomonas aeruginosa N002 reveals its genetic adaptation for crude oil degradation. *Genomics* **2015**, *105*, 182–190. [CrossRef]

19. Chen, S.; Chen, W.; Xingxing, P.; Ma, Y.; He, C.; Li, Y.; Huang, C.; Chen, F. Genome Sequence and Metabolic Analysis of a Fluoranthene-Degrading Strain Pseudomonas aeruginosa DN1. *Front. Microbiol.* **2018**, *9*, 2595. [CrossRef]

20. Wang, M.Q.; Wang, Z.; Yu, L.N.; Zhang, C.S.; Bi, J.; Sun, J. *Pseudomonas qingdaonensis* sp. nov., an aflatoxin-degrading bacterium, isolated from peanut rhizospheric soil. *Arch. Microbiol.* **2019**, *201*, 673–678. [CrossRef]

21. Mulet, M.; Lalucat, J.; García-Valdés, E. DNA sequence-based analysis of the Pseudomonas species. *Environ. Microbiol.* **2010**, *12*, 1513–1530. [CrossRef]

22. Kang, S.-M.; Asaf, S.; Khan, A.L.; Lubna; Khan, A.; Mun, B.-G.; Khan, M.A.; Gul, H.; Lee, I.-J. Complete Genome Sequence of Pseudomonas psychrotolerans CS51, a Plant Growth-Promoting Bacterium, Under Heavy Metal Stress Conditions. *Microorganisms* **2020**, *8*, 382. [CrossRef]

23. Khatri, S.; Sazinas, P.; Shivay, Y.S.; Sharma, S.; Jelsbak, L. Complete Genome Sequence of *Pseudomonas* sp. Strain SK, Isolated from Organic Wheat Rhizosphere. *Microbiol. Resour. Announc.* **2021**, *9*, e00510-20. [CrossRef]

24. Andrés-Barrao, C.; Lafi, F.F.; Alam, I.; de Zélicourt, A.; Eida, A.A.; Bokhari, A.; Alzubaidy, H.; Bajic, V.B.; Hirt, H.; Saad, M.M. Complete genome sequence analysis of *Enterobacter* sp. SA187, a plant multi-stress tolerance promoting endophytic bacterium. *Front. Microbiol.* **2017**, *8*, 2023. [CrossRef] [PubMed]

25. Szczerba, H.; Komoń-Janczara, E.; Krawczyk, M.; Dudziak, K.; Nowak, A.; Kuzdraliński, A.; Waśko, A.; Targoński, Z. Genome analysis of a wild rumen bacterium Enterobacter aerogenes LU2-a novel bio-based succinic acid producer. *Sci. Rep.* **2020**, *10*, 1986. [CrossRef]

26. Eida, A.A.; Bougouffa, S.; L'Haridon, F.; Alam, I.; Weisskopf, L.; Bajic, V.B.; Saad, M.M.; Hirt, H. Genome Insights of the Plant-Growth Promoting Bacterium Cronobacter muytjensii JZ38 With Volatile-Mediated Antagonistic Activity Against Phytophthora infestans. *Front. Microbiol.* **2020**, *11*, 369. [CrossRef]

27. Martínez-García, P.M.; Ruano-Rosa, D.; Schilirò, E.; Prieto, P.; Ramos, C.; Rodríguez-Palenzuela, P.; Mercado-Blanco, J. Complete genome sequence of Pseudomonas fluorescens strain PICF7, an indigenous root endophyte from olive (*Olea europaea* L.) and effective biocontrol agent against Verticillium dahliae. *Stand. Genom. Sci.* **2015**, *10*, 10. [CrossRef]

28. Duan, J.; Jiang, W.; Cheng, Z.; Heikkila, J.J.; Glick, B.R. The Complete Genome Sequence of the Plant Growth-Promoting *Bacterium pseudomonas* sp. UW4. *PLoS ONE* **2013**, *8*, e58640. [CrossRef]

29. Li, H.B.; Singh, R.K.; Singh, P.; Song, Q.Q.; Xing, Y.X.; Yang, L.T.; Li, Y.R. Genetic diversity of nitrogen-fixing and plant growth promoting Pseudomonas species isolated from sugarcane rhizosphere. *Front. Microbiol.* **2017**, *8*, 1–20. [CrossRef]

30. Ma, Y.; Zhang, Q.L.; Yang, Z.M.; Li, Y.; Yan, Y.L.; Ping, S.Z.; Zhang, L.W.; Lin, M.; Lu, W. Identification of the nitrogen-fixing Pseudomonas stutzeri major flagellar gene regulator FleQ and its role in biofilm formation and root colonization. *J. Integr. Agric.* **2016**, *15*, 339–348. [CrossRef]

31. Yan, Y.; Yang, J.; Dou, Y.; Chen, M.; Ping, S.; Peng, J.; Lu, W.; Zhang, W.; Yao, Z.; Li, H.; et al. Nitrogen fixation island and rhizosphere competence traits in the genome of root-associated Pseudomonas stutzeri A1501. *Proc. Natl. Acad. Sci. USA* **2008**, *105*, 7564–7569. [CrossRef]

32. Dos Santos, P.C.; Johnson, D.C.; Ragle, B.E.; Unciuleac, M.C.; Dean, D.R. Controlled expression of nif and isc iron-sulfur protein maturation components reveals target specificity and limited functional replacement between the two systems. *J. Bacteriol.* **2007**, *189*, 2854–2862. [CrossRef] [PubMed]

33. Tokumoto, U.; Kitamura, S.; Fukuyama, K.; Takahashi, Y. Interchangeability and distinct properties of bacterial Fe-S cluster assembly systems: Functional replacement of the isc and suf operons in Escherichia coli with the nifSU-like operon from Helicobacter pylori. *J. Biochem.* **2004**, *136*, 199–209. [CrossRef] [PubMed]

34. Dai, Z.; Liu, G.; Chen, H.; Chen, C.; Wang, J.; Ai, S.; Wei, D.; Li, D.; Ma, B.; Tang, C.; et al. Long-term nutrient inputs shift soil microbial functional profiles of phosphorus cycling in diverse agroecosystems. *ISME J.* **2020**, *14*, 757–770. [CrossRef]

35. Hoelzle, K.; Peter, S.; Sidler, M.; Kramer, M.M.; Wittenbrink, M.M.; Felder, K.M.; Hoelzle, L.E. Inorganic pyrophosphatase in uncultivable hemotrophic mycoplasmas: Identification and properties of the enzyme from Mycoplasma suis. *BMC Microbiol.* **2010**, *10*. [CrossRef]

36. Albi, T.; Serrano, A. Two exopolyphosphatases with distinct molecular architectures and substrate specificities from the thermophilic green-sulfur bacterium Chlorobium tepidum TLS. *Microbiology* **2014**, *160*, 2067–2078. [CrossRef] [PubMed]

37. Gebhard, S.; Ekanayaka, N.; Cook, G.M. The low-affinity phosphate transporter PitA is dispensable for in vitro growth of Mycobacterium smegmatis. *BMC Microbiol.* **2009**, *9*, 1–7. [CrossRef]

38. Hsieh, Y.-J.; Wanner, B.L. Global regulation by the seven-component Pi signaling system. *Curr. Opin. Microbiol.* **2010**, *13*, 198–203. [CrossRef]

39. Sekine, M.; Tanikawa, S.; Omata, S.; Saito, M.; Fujisawa, T.; Tsukatani, N.; Tajima, T.; Sekigawa, T.; Kosugi, H.; Matsuo, Y.; et al. Sequence analysis of three plasmids harboured in Rhodococcus erythropolis strain PR4. *Environ. Microbiol.* **2006**, *8*, 334–346. [CrossRef]

40. Coleman, N.V.; Wilson, N.L.; Barry, K.; Brettin, T.S.; Bruce, D.C.; Copeland, A.; Dalin, E.; Detter, J.C.; del Rio, T.G.; Goodwin, L.A.; et al. Genome sequence of the ethene-and vinyl chloride-oxidizing actinomycete *Nocardioides* sp. strain JS614. *J. Bacteriol.* **2011**, *193*, 3399–3400. [CrossRef]

41. Copeland, A.; Lapidus, A.; del Rio, T.G.; Nolan, M.; Lucas, S.; Chen, F.; Tice, H.; Cheng, J.F.; Bruce, D.; Goodwin, L.; et al. Complete genome sequence of Catenulispora acidiphila type strain (ID 139908T). *Stand. Genom. Sci.* **2009**, *1*, 119–125. [CrossRef]

42. Normand, P.; Lapierre, P.; Tisa, L.S.; Gogarten, J.P.; Alloisio, N.; Bagnarol, E.; Bassi, C.A.; Berry, A.M.; Bickhart, D.M.; Choisne, N.; et al. Genome characteristics of facultatively symbiotic *Frankia* sp. strains reflect host range and host plant biogeography. *Genome Res.* **2007**, *17*, 7–15. [CrossRef] [PubMed]

43. Marzan, L.W.; Shimizu, K. Metabolic regulation of Escherichia coli and its phoB and phoR genes knockout mutants under phosphate and nitrogen limitations as well as at acidic condition. *Microb. Cell Fact.* **2011**, *10*, 1–15. [CrossRef] [PubMed]

44. Lubin, E.A.; Henry, J.T.; Fiebig, A.; Crosson, S.; Laub, M.T. Identification of the PhoB regulon and role of PhoU in the phosphate starvation response of Caulobacter crescentus. *J. Bacteriol.* **2016**, *198*, 187–200. [CrossRef]

45. Gigolashvili, T.; Kopriva, S. Transporters in plant sulfur metabolism. *Front. Plant Sci.* **2014**, *5*, 1–16. [CrossRef]

46. Gahan, J.; Schmalenberger, A. The role of bacteria and mycorrhiza in plant sulfur supply. *Front. Plant Sci.* **2014**, *5*, 1–7. [CrossRef] [PubMed]

47. Asaf, S.; Khan, A.L.; Khan, M.A.; Al-Harrasi, A.; Lee, I.J. Complete genome sequencing and analysis of endophytic *Sphingomonas* sp. LK11 and its potential in plant growth. *3 Biotech* **2018**, *8*, 389. [CrossRef] [PubMed]

48. Zou, H.; Zhang, N.N.; Pan, Q.; Zhang, J.H.; Chen, J.; Wei, G.H. Hydrogen sulfide promotes nodulation and nitrogen fixation in soybean–rhizobia symbiotic system. *Mol. Plant Microbe Interact.* **2019**, *32*, 972–985. [CrossRef]

49. Shariati, J.V.; Malboobi, M.A.; Tabrizi, Z.; Tavakol, E. Comprehensive genomic analysis of a plant growth-promoting rhizobacterium Pantoea agglomerans strain P5. *Sci. Rep.* **2017**, 15610. [CrossRef]

50. Rout, G.R.; Sahoo, S. Role of Iron in Plant Growth and Metabolism. *Rev. Agric. Sci.* **2015**, *3*, 1–24. [CrossRef]

51. Mirus, O.; Strauss, S.; Nicolaisen, K.; von Haeseler, A.; Schleiff, E. TonB-dependent transporters and their occurrence in cyanobacteria. *BMC Biol.* **2009**, *7*, 68. [CrossRef]

52. Johnson, G.V.; Lopez, A.; La Valle Foster, N. Reduction and transport of Fe from siderophores. *Plant Soil* **2002**, *241*, 27–33. [CrossRef]

53. Fernàndez, V.; Ebert, G.; Winkelmann, G. The use of microbial siderophores for foliar iron application studies. *Plant Soil* **2005**, *272*, 245–252. [CrossRef]

54. Crowley, D.E.; Römheld, V.; Marschner, H.; Szaniszlo, P.J. Root-microbial effects on plant iron uptake from siderophores and phytosiderophores. *Plant Soil* **1992**, *142*, 1–7. [CrossRef]

55. Rajkumar, M.; Ae, N.; Prasad, M.N.V.; Freitas, H. Potential of siderophore-producing bacteria for improving heavy metal phytoextraction. *Trends Biotechnol.* **2010**, *28*, 142–149. [CrossRef] [PubMed]

56. Guo, J.K.; Muhammad, H.; Lv, X.; Wei, T.; Ren, X.H.; Jia, H.L.; Atif, S.; Hua, L. Prospects and applications of plant growth promoting rhizobacteria to mitigate soil metal contamination: A review. *Chemosphere* **2020**, *246*, 125OK823. [CrossRef] [PubMed]

57. Khalid, A.; Tahir, S.; Arshad, M.; Zahir, Z.A. Relative efficiency of rhizobacteria for auxin biosynthesis in rhizosphere and non-rhizosphere soils. *Aust. J. Soil Res.* **2004**, *42*, 921–926. [CrossRef]

58. de Souza, R.; Beneduzi, A.; Ambrosini, A.; da Costa, P.B.; Meyer, J.; Vargas, L.K.; Schoenfeld, R.; Passaglia, L.M.P. The effect of plant growth-promoting rhizobacteria on the growth of rice (*Oryza sativa* L.) cropped in southern Brazilian fields. *Plant Soil* **2013**, *366*, 585–603. [CrossRef]

59. Suarez, C.; Ratering, S.; Hain, T.; Fritzenwanker, M.; Goesmann, A.; Blom, J.; Chakraborty, T.; Bunk, B.; Spröer, C.; Overmann, J.; et al. Complete genome sequence of the plant growth-promoting bacterium hartmannibacter diazotrophicus strain E19T. *Int. J. Genom.* **2019**, *2019*. [CrossRef]

60. McDonnell, L.; Plett, J.M.; Andersson-Gunneras, S.; Kozela, C.; Dugardeyn, J.; Van Der Straeten, D.; Glick, B.R.; Sundberg, B.; Regan, S. Ethylene levels are regulated by a plant encoded 1-aminocyclopropane-1- carboxylic acid deaminase. *Physiol. Plant.* **2009**, *136*, 94–109. [CrossRef]

61. Todorovic, B.; Glick, B.R. The interconversion of ACC deaminase and D-cysteine desulfhydrase by directed mutagenesis. *Planta* **2008**, *229*, 193–205. [CrossRef]

62. Penrose, D.M.; Glick, B.R. Methods for isolating and characterizing ACC deaminase-containing plant growth-promoting rhizobacteria. *Physiol. Plant.* **2003**, *118*, 10–15. [CrossRef] [PubMed]

63. Hong, S.H.; Ryu, H.W.; Kim, J.; Cho, K.S. Rhizoremediation of diesel-contaminated soil using the plant growth-promoting rhizobacterium *Gordonia* sp. S2RP-17. *Biodegradation* **2011**, *22*, 593–601. [CrossRef]

64. Grobelak, A.; Kokot, P.; Świątek, J.; Jaskulak, M.; Rorat, A. Bacterial ACC Deaminase Activity in Promoting Plant Growth on Areas Contaminated with Heavy Metals. *J. Ecol. Eng.* **2018**, *19*, 150–157. [CrossRef]

65. Kandel, S.L.; Joubert, P.M.; Doty, S.L. Bacterial endophyte colonization and distribution within plants. *Microorganisms* **2017**, *5*, 77. [CrossRef]

66. Pérez-Montaño, F.; Alías-Villegas, C.; Bellogín, R.A.; Del Cerro, P.; Espuny, M.R.; Jiménez-Guerrero, I.; López-Baena, F.J.; Ollero, F.J.; Cubo, T. Plant growth promotion in cereal and leguminous agricultural important plants: From microorganism capacities to crop production. *Microbiol. Res.* **2014**, *169*, 325–336. [CrossRef] [PubMed]

67. Tripathi, M.; Munot, H.P.; Shouche, Y.; Meyer, J.M.; Goel, R.; Journal, A.I. Isolation and Functional Characterization of Siderophore-Producing Lead-and Cadmium-Resistant Pseudomonas putida KNP9 Current Microbiology. *Curr. Microbiol.* **2005**, *50*, 233–237. [CrossRef] [PubMed]

68. Caracciolo, A.B.; Terenzi, V.; Saccà, L.; Manici, L.M. microorganisms Rhizosphere Microbial Communities and Heavy Metals. *Microorganisms* **2021**, *9*, 1462. [CrossRef]

69. Ducret, V.; Gonzalez, M.R.; Leoni, S.; Valentini, M.; Perron, K. The CzcCBA Efflux System Requires the CadA P-Type ATPase for Timely Expression Upon Zinc Excess in Pseudomonas aeruginosa. *Front. Microbiol.* **2020**, *11*, 911. [CrossRef]

70. Fernando, D.M.; Kumar, A. Resistance-Nodulation-Division multidrug efflux pumps in Gram-negative bacteria: Role in virulence. *Antibiotics* **2013**, *2*, 163–181. [CrossRef]

71. Legatzki, A.; Grass, G.; Anton, A.; Rensing, C.; Nies, D.H. Interplay of the Czc system and two P-type ATPases in conferring metal resistance to Ralstonia metallidurans. *J. Bacteriol.* **2003**, *185*, 4354–4361. [CrossRef]

72. Bondarczuk, K.; Piotrowska-Seget, Z. Molecular basis of active copper resistance mechanisms in Gram-negative bacteria. *Cell Biol. Toxicol.* **2013**, *29*, 397–405. [CrossRef]

73. González-Guerrero, M.; Raimunda, D.; Cheng, X.; Argüello, J.M. Distinct functional roles of homologous Cu+ efflux ATPases in Pseudomonas aeruginosa. *Mol. Microbiol.* **2010**, *78*, 1246–1258. [CrossRef] [PubMed]

74. Marrero, K.; Sánchez, A.; González, L.J.; Ledón, T.; Rodríguez-Ulloa, A.; Castellanos-Serra, L.; Pérez, C.; Fando, R. Periplasmic proteins encoded by VCA0261-0260 and VC2216 genes together with copA and cueR products are required for copper tolerance but not for virulence in Vibrio cholerae. *Microbiology* **2012**, *158*, 2005–2016. [CrossRef] [PubMed]

75. Osman, D.; Waldron, K.J.; Denton, H.; Taylor, C.M.; Grant, A.J.; Mastroeni, P.; Robinson, N.J.; Cavet, J.S. Copper homeostasis in Salmonella is atypical and copper-CueP is a major periplasmic metal complex. *J. Biol. Chem.* **2010**, *285*, 25259–25268. [CrossRef]

76. Outten, F.W.; Huffman, D.L.; Hale, J.A.; O'Halloran, T.V. The Independent cue and cus Systems Confer Copper Tolerance during Aerobic and Anaerobic Growth in Escherichia coli. *J. Biol. Chem.* **2001**, *276*, 30670–30677. [CrossRef] [PubMed]

77. Ahemad, M. Bacterial mechanisms for Cr(VI) resistance and reduction: An overview and recent advances. *Folia Microbiol.* **2014**, *59*, 321–332. [CrossRef] [PubMed]

78. Gonzalez, C.F.; Aekerley, D.F.; Lynch, S.V.; Matin, A. ChrR, a soluble quinone reductase of Pseudomonas putida that defends against H2O2. *J. Biol. Chem.* **2005**, *280*, 22590–22595. [CrossRef]

79. Ben Fekih, I.; Zhang, C.; Li, Y.P.; Zhao, Y.; Alwathnani, H.A.; Saquib, Q.; Rensing, C.; Cervantes, C. Distribution of arsenic resistance genes in prokaryotes. *Front. Microbiol.* **2018**, *9*, 2473. [CrossRef]

80. Chen, J.; Bhattacharjee, H.; Rosen, B.P. ArsH is an organoarsenical oxidase that confers resistance to trivalent forms of the herbicide monosodium methylarsenate and the poultry growth promoter roxarsone. *Mol. Microbiol.* **2015**, *96*, 1042–1052. [CrossRef]

81. Kiyono, M.; Sone, Y.; Nakamura, R.; Pan-Hou, H.; Sakabe, K. The MerE protein encoded by transposon Tn21 is a broad mercury transporter in Escherichia coli. *FEBS Lett.* **2009**, *583*, 1127–1131. [CrossRef] [PubMed]

82. Spaniol, V.; Bernhard, S.; Aebi, C. Moraxella catarrhalis AcrAB-OprM efflux pump contributes to antimicrobial resistance and is enhanced during cold shock response. *Antimicrob. Agents Chemother.* **2015**, *59*, 1886–1894. [CrossRef] [PubMed]

83. Whitney, J.C.; Howell, P.L. Synthase-dependent exopolysaccharide secretion in Gram-negative bacteria. *Trends Microbiol.* **2013**, *21*, 63–72. [CrossRef]

84. Nilsson, M.; Chiang, W.C.; Fazli, M.; Gjermansen, M.; Givskov, M.; Tolker-Nielsen, T. Influence of putative exopolysaccharide genes on Pseudomonas putida KT2440 biofilm stability. *Environ. Microbiol.* **2011**, *13*, 1357–1369. [CrossRef] [PubMed]

85. Lee, K.; Lim, E.J.; Kim, K.S.; Huang, S.L.; Veeranagouda, Y.; Rehm, B.H.A. An alginate-like exopolysaccharide biosynthesis gene cluster involved in biofilm aerial structure formation by Pseudomonas alkylphenolia. *Appl. Microbiol. Biotechnol.* **2014**, *98*, 4137–4148. [CrossRef]

86. Gupta, P.; Diwan, B. Bacterial Exopolysaccharide mediated heavy metal removal: A Review on biosynthesis, mechanism and remediation strategies. *Biotechnol. Rep.* **2017**, *13*, 58–71. [CrossRef]

87. Sönmez, M.; Ficai, A.; Ficai, D.; Trusca, R.; Andronescu, E. Alginate/cellulose composite beads for environmental applications. *UPB Sci. Bull. Ser. B Chem. Mater. Sci.* **2016**, *78*, 165–176.

88. Liang, Y.; Chen, J.Q.; Mei, J.; Chang, J.J.; Wang, Q.Y.; Wan, G.S.; Yin, B.Y. Characterization of Cu and Cd biosorption by *Pseudomonas* sp. strain DC-B3 isolated from metal mine soil. *Int. J. Environ. Sci. Technol.* **2018**, *16*, 4035–4046. [CrossRef]

89. Xu, S.; Xing, Y.; Liu, S.; Hao, X.; Chen, W.; Huang, Q. Characterization of Cd2+ biosorption by *Pseudomonas* sp. strain 375, a novel biosorbent isolated from soil polluted with heavy metals in Southern China. *Chemosphere* **2020**, *240*, 124893. [CrossRef]

90. Taran, O.; Patel, V.; Lynn, D.G. Small molecule reaction networks that model the ROS dynamics of the rhizosphere. *Chem. Commun.* **2019**, *55*, 3602–3605. [CrossRef]

91. Wu, X.; Monchy, S.; Taghavi, S.; Zhu, W.; Ramos, J.; Van Der Lelie, D. Comparative genomics and functional analysis of niche-specific adaptation in Pseudomonas putida. *FEMS Microbiol. Rev.* **2011**, *35*, 299–323. [CrossRef]

92. Chen, Q.; Li, J.; Liu, M.; Sun, H.; Bao, M. Study on the biodegradation of crude oil by free and immobilized bacterial consortium in marine environment. *PLoS ONE* **2017**, *12*, e0174445. [CrossRef] [PubMed]

93. Muriel-Millán, L.F.; Rodríguez-Mejía, J.L.; Godoy-Lozano, E.E.; Rivera-Gómez, N.; Gutierrez-Rios, R.M.; Morales-Guzmán, D.; Trejo-Hernández, M.R.; Estradas-Romero, A.; Pardo-López, L. Functional and Genomic Characterization of a Pseudomonas aeruginosa Strain Isolated From the Southwestern Gulf of Mexico Reveals an Enhanced Adaptation for Long-Chain Alkane Degradation. *Front. Mar. Sci.* **2019**, *6*, 572. [CrossRef]

94. Mahjoubi, M.; Aliyu, H.; Neifar, M.; Cappello, S.; Chouchane, H.; Souissi, Y.; Masmoudi, A.S.; Cowan, D.A.; Cherif, A. Genomic characterization of a polyvalent hydrocarbonoclastic bacterium *Pseudomonas* sp. strain BUN14. *Sci. Rep.* **2021**, *11*, 8124. [CrossRef]

95. Phillips, L.A.; Germida, J.J.; Farrell, R.E.; Greer, C.W. Hydrocarbon degradation potential and activity of endophytic bacteria associated with prairie plants. *Soil Biol. Biochem.* **2008**, *40*, 3054–3064. [CrossRef]

96. Andria, V.; Reichenauer, T.G.; Sessitsch, A. Expression of alkane monooxygenase (alkB) genes by plant-associated bacteria in the rhizosphere and endosphere of Italian ryegrass (*Lolium multiflorum* L.) grown in diesel contaminated soil. *Environ. Pollut.* **2009**, *157*, 3347–3350. [CrossRef]

97. Feng, L.; Wang, W.; Cheng, J.; Ren, Y.; Zhao, G.; Gao, C.; Tang, Y.; Liu, X.; Han, W.; Peng, X.; et al. Genome and proteome of long-chain alkane degrading Geobacillus thermodenitrificans NG80-2 isolated from a deep-subsurface oil reservoir. *Proc. Natl. Acad. Sci. USA* **2007**, *104*, 5602–5607. [CrossRef]

98. Tourova, T.P.; Sokolova, D.S.; Semenova, E.M.; Shumkova, E.S.; Korshunova, A.V.; Babich, T.L.; Poltaraus, A.B.; Nazina, T.N. Detection of n-alkane biodegradation genes alkB and ladA in thermophilic hydrocarbon-oxidizing bacteria of the genera Aeribacillus and Geobacillus. *Microbiology* **2016**, *85*, 693–707. [CrossRef]

99. Ji, Y.; Mao, G.; Wang, Y.; Bartlam, M. Structural insights into diversity and n-alkane biodegradation mechanisms of alkane hydroxylases. *Front. Microbiol.* **2013**, *4*, 58. [CrossRef]

100. Meng, L.; Bao, M.; Sun, P. Construction of long-chain alkane degrading bacteria and its application in bioremediation of crude oil pollution. *Int. J. Biol. Macromol.* **2018**, *119*, 524–532. [CrossRef]

101. Fuchs, G.; Boll, M.; Heider, J. Microbial degradation of aromatic compounds—from one strategy to four. *Nat. Rev. Microbiol.* **2011**, *9*, 803–816. [CrossRef] [PubMed]

102. Li, D.; Yan, Y.; Ping, S.; Chen, M.; Zhang, W.; Li, L.; Lin, W.; Geng, L.; Liu, W.; Lu, W.; et al. Genome-wide investigation and functional characterization of the β-ketoadipate pathway in the nitrogen-fixing and root-associated bacterium Pseudomonas stutzeriA1501. *BMC Microbiol.* **2010**, *10*, 36. [CrossRef]

103. Nogales, J.; García, J.L.; Díaz, E. Degradation of Aromatic Compounds in Pseudomonas: A Systems Biology View. In *Aerobic Utilization of Hydrocarbons, Oils and Lipids*; Rojo, F., Ed.; Springer International Publishing: Cham, Switzerland, 2017; pp. 1–49; ISBN 978-3-319-39782-5.

104. Alejandro-Marín, C.M.; Bosch, R.; Nogales, B. Comparative genomics of the protocatechuate branch of the β-ketoadipate pathway in the Roseobacter lineage. *Mar. Genom.* **2014**, *17*, 25–33. [CrossRef] [PubMed]

105. Tikariha, H.; Pal, R.R.; Qureshi, A.; Kapley, A.; Purohit, H.J. In silico analysis for prediction of degradative capacity of Pseudomonas putida SF1. *Gene* **2016**, *591*, 382–392. [CrossRef] [PubMed]

106. Méndez, V.; Agulló, L.; González, M.; Seeger, M. The homogentisate and homoprotocatechuate central pathways are involved in 3- and 4-hydroxyphenylacetate degradation by Burkholderia xenovorans LB400. *PLoS ONE* **2011**, *6*. [CrossRef]

107. Pacwa-Płociniczak, M.; Płaza, G.A.; Poliwoda, A.; Piotrowska-Seget, Z. Characterization of hydrocarbon-degrading and biosurfactant-producing *Pseudomonas* sp. P-1 strain as a potential tool for bioremediation of petroleum-contaminated soil. *Environ. Sci. Pollut. Res.* **2014**, *21*. [CrossRef]

108. Guo, G.; Tian, F.; Ding, K.; Wang, L.; Liu, T.; Yang, F. Effect of a bacterial consortium on the degradation of polycyclic aromatic hydrocarbons and bacterial community composition in Chinese soils. *Int. Biodeterior. Biodegradation* **2017**, *123*, 56–62. [CrossRef]

109. Chlebek, D.; Pinski, A.; Żur, J.; Michalska, J.; Hupert-Kocurek, K. Genome Mining and Evaluation of the Biocontrol Potential of Pseudomonas fluorescens BRZ63, a New Endophyte of Oilseed Rape (*Brassica napus* L.) against Fungal Pathogens. *Int. J. Mol. Sci.* **2020**, *21*, 8740. [CrossRef] [PubMed]

110. Cheng, T.; Liang, J.; He, J.; Hu, X.; Ge, Z.; Liu, J. A novel rhamnolipid-producing pseudomonas aeruginosa zs1 isolate derived from petroleum sludge suitable for bioremediation. *AMB Express* **2017**, *7*, 1–14. [CrossRef]

111. Omoboye, O.O.; Geudens, N.; Duban, M.; Chevalier, M.; Flahaut, C.; Martins, J.C.; Leclère, V.; Oni, F.E.; Höfte, M. *Pseudomonas* sp. COW3 produces new bananamide-type cyclic lipopeptides with antimicrobial activity against *Pythium myriotylum* and *Pyricularia oryzae*. *Molecules* **2019**, *24*, 4170. [CrossRef]

112. Zhang, J.; Xue, Q.; Gao, H.; Lai, H.; Wang, P. Production of lipopeptide biosurfactants by Bacillus atrophaeus 5-2a and their potential use in microbial enhanced oil recovery. *Microb. Cell Fact.* **2016**, *15*, 168. [CrossRef]

113. Gutiérrez-Chávez, C.; Benaud, N.; Ferrari, B.C. The ecological roles of microbial lipopeptides: Where are we going? *Comput. Struct. Biotechnol. J.* **2021**, *19*, 1400–1413. [CrossRef] [PubMed]

114. Viramontes-Ramos, S.; Portillo-Ruiz, M.C.; de Lourdes Ballinas-Casarrubias, M.; Torres-Muñoz, J.V.; Rivera-Chavira, B.E.; Nevárez-Moorillón, G.V. Selection of biosurfactan/bioemulsifier-producing bacteria from hydrocarbon-contaminated soil. *Braz. J. Microbiol.* **2010**, *41*, 668–675. [CrossRef]

115. Saleh, S.S.; Glick, B.R. Involvement of gacS and rpoS in enhancement of the plant growth-promoting capabilities of Enterobacter cloacae CAL2 and UW4. *Can. J. Microbiol.* **2001**, *47*, 698–705. [CrossRef] [PubMed]

116. Bradford, M.M. A rapid and sensitive method for the quantitation of microgram quantities of protein utilizing the principle of protein-dye binding. *Anal. Biochem.* **1976**, *72*, 248–254. [CrossRef]

117. Pointing, S.B. Qualitative methods for the determination of lignocellulolytic enzyme production by tropical fungi. *Fungal Divers.* **1999**, *2*, 17–33.

118. Schwyn, B.; Neilands, J.B. Universal chemical assay for the detection and determination of siderophores. *Anal. Biochem.* **1987**, *160*, 47–56. [CrossRef]

119. Bric, J.M.; Bostock, R.M.; Silverstone, S.E. Rapid in situ assay for indoleacetic acid production by bacteria immobilized on a nitrocellulose membrane. *Appl. Environ. Microbiol.* **1991**, *57*, 535–538. [CrossRef] [PubMed]

120. Cappuccino, J.C.; Sherman, N. *Microbiology: A Laboratory Manual*, 3rd ed.; Benjamin Cummings Publisher: New York, NY, USA, 1992.

121. Nautiyal, C.S. An efficient microbiological growth medium for screening phosphate solubilizing microorganisms. *FEMS Microbiol. Lett.* **1999**, *170*, 265–270. [CrossRef]

122. Lorck, H. Production of Hydrocyanic Acid by Bacteria. *Physiol. Plant.* **1948**, *1*, 142–146. [CrossRef]

123. Pacwa-Płociniczak, M.; Płociniczak, T.; Iwan, J.; Zarska, M.; Chorazewski, M.; Dzida, M.; Piotrowska-Seget, Z. Isolation of hydrocarbon-degrading and biosurfactant-producing bacteria and assessment their plant growth-promoting traits. *J. Environ. Manag.* **2016**, *168*, 175–184. [CrossRef]

124. Ptaszek, N.; Pacwa-Płociniczak, M.; Noszczyńska, M.; Płociniczak, T. Comparative Study on Multiway Enhanced Bio- and Phytoremediation of Aged Petroleum-Contaminated Soil. *Agronomy* **2020**, *10*, 947. [CrossRef]

125. Iverson, W.G.; Millis, N.F. A Method for the Detection of Starch Hydrolysis by Bacteria. *J. Appl. Bacteriol.* **1974**, *37*, 443–446. [CrossRef]

126. Hidayat, I. Characteristics of the peat soil *Bacilllus* sp. *Berk. Penelit. Hayati* **2004**, *10*, 31–35. [CrossRef]

127. Peck, H.D.; Gest, H. Formic dehydrogenase and the hydrogenlyase enzyme complex in coli-aerogenes bacteria. *J. Bacteriol.* **1957**, *73*, 706–721. [CrossRef]

128. Taylor, J.J.; Whitby, J.L. Pseudomonas Pyocyanea and the Arginine Dihydrolase System. *J. Clin. Pathol.* **1964**, *17*, 122–125. [CrossRef]

129. Christensen, W.B. Urea Decomposition as a Means of Differentiating Proteus and Paracolon Cultures from Each Other and from Salmonella and Shigella Types. *J. Bacteriol.* **1946**, *52*, 461–466. [CrossRef]

130. King, E.O.; Ward, M.K.; Raney, D.E. Two simple media for the demonstration of pyocyanin and fluorescin. *J. Lab. Clin. Med.* **1954**, *44*, 301–307. [PubMed]

131. Piotrowska-Seget, Z.; Cycoń, M.; Kozdrój, J. Metal-tolerant bacteria occurring in heavily polluted soil and mine spoil. *Appl. Soil Ecol.* **2005**, *28*, 237–246. [CrossRef]

132. Huerta-Cepas, J.; Szklarczyk, D.; Heller, D.; Hernández-Plaza, A.; Forslund, S.K.; Cook, H.; Mende, D.R.; Letunic, I.; Rattei, T.; Jensen, L.J.; et al. EggNOG 5.0: A hierarchical, functionally and phylogenetically annotated orthology resource based on 5090 organisms and 2502 viruses. *Nucleic Acids Res.* **2019**, *47*, D309–D314. [CrossRef]

133. Davis, J.J.; Wattam, A.R.; Aziz, R.K.; Brettin, T.; Butler, R.; Butler, R.M.; Chlenski, P.; Conrad, N.; Dickerman, A.; Dietrich, E.M.; et al. The PATRIC Bioinformatics Resource Center: Expanding data and analysis capabilities. *Nucleic Acids Res.* **2020**, *48*. [CrossRef]

134. Kanehisa, M.; Sato, Y.; Kawashima, M.; Furumichi, M.; Tanabe, M. KEGG as a reference resource for gene and protein annotation. *Nucleic Acids Res.* **2016**, *44*, D457–D462. [CrossRef] [PubMed]

135. Wu, S.; Zhu, Z.; Fu, L.; Niu, B.; Li, W. WebMGA: A customizable web server for fast metagenomic sequence analysis. *BMC Genomics* **2011**, *12*, 444. [CrossRef] [PubMed]

136. Blin, K.; Shaw, S.; Steinke, K.; Villebro, R.; Ziemert, N.; Lee, S.Y.; Medema, M.H.; Weber, T. AntiSMASH 5.0: Updates to the secondary metabolite genome mining pipeline. *Nucleic Acids Res.* **2019**, *47*, W81–W87. [CrossRef]

137. Zhou, Y.; Liang, Y.; Lynch, K.H.; Dennis, J.J.; Wishart, D.S. PHAST: A Fast Phage Search Tool. *Nucleic Acids Res.* **2011**, *39*, 347–352. [CrossRef]

138. Furmanczyk, E.M.; Kaminski, M.A.; Lipinski, L.; Dziembowski, A.; Sobczak, A. *Pseudomonas laurylsulfatovorans* sp. nov., sodium dodecyl sulfate degrading bacteria, isolated from the peaty soil of a wastewater treatment plant. *Syst. Appl. Microbiol.* **2018**, *41*, 348–354. [CrossRef]

139. Kumar, S.; Stecher, G.; Li, M.; Knyaz, C.; Tamura, K. MEGA X: Molecular evolutionary genetics analysis across computing platforms. *Mol. Biol. Evol.* **2018**, *35*, 1547–1549. [CrossRef]

140. Yoon, S.H.; Ha, S.; Lim, J.; Kwon, S.; Chun, J. A large-scale evaluation of algorithms to calculate average nucleotide identity. *Antonie van Leeuwenhoek/Int. J. Gen. Mol. Microbiol.* **2017**, *110*, 1281–1286. [CrossRef] [PubMed]

141. Ha, S.M.; Kim, C.K.; Roh, J.; Byun, J.H.; Yang, S.J.; Bin Choi, S.; Chun, J.; Yong, D. Application of the whole genome-based bacterial identification system, TRUEBAC ID, using clinical isolates that were not identified with three matrix-assisted laser desorption/ionization time-of-flight mass spectrometry (MALDI-TOF MS) systems. *Ann. Lab. Med.* **2019**, *39*, 530–536. [CrossRef]

142. Richter, M.; Rosselló-Móra, R.; Glöckner, F.O.; Rg Peplies, J. JSpeciesWS: A web server for prokaryotic species circumscription based on pairwise genome comparison. *Bioinformatics* **2016**, *32*, 929–931. [CrossRef]

143. Rathnayake, I.V.N.; Megharaj, M.; Krishnamurti, G.S.R.; Bolan, N.S.; Naidu, R. Heavy metal toxicity to bacteria—Are the existing growth media accurate enough to determine heavy metal toxicity? *Chemosphere* **2013**, *90*, 1195–1200. [CrossRef] [PubMed]

144. Manogaran, M.; Shukor, M.Y.; Yasid, N.A.; Khalil, K.A.; Ahmad, S.A. Optimisation of culture composition for glyphosate degradation by Burkholderia vietnamiensis strain AQ5-12. *3 Biotech* **2018**, *8*, 108. [CrossRef] [PubMed]